Progress in Oceanography 162 (2018) 187–201

Contents lists available at ScienceDirect

Progress in Oceanography

journal homepage: www.elsevier.com/locate/pocean

Review

Seasonal and inter-annual variations of dissolved oxygen in the northwestern Mediterranean Sea (DYFAMED site)

Laurent Coppola[a,*], Louis Legendre[a], Dominique Lefevre[b], Louis Prieur[a], Vincent Taillandier[a], Emilie Diamond Riquier[a]

[a] Sorbonne Université, CNRS, Laboratoire d'Océanographie de Villefranche, LOV, F-06230 Villefranche-sur-Mer, France
[b] Aix-Marseille Université, Mediterranean Institute of Oceanography (MIO), 13288 Marseille Cedex 9, France

ARTICLE INFO

Keywords:
DYFAMED
Ligurian Sea
Dissolved oxygen
Time series
Dense water formation
Net community production

ABSTRACT

Dissolved oxygen (O_2) is a relevant tracer to interpret variations of both water mass properties in the open ocean and biological production in the surface layer of both coastal and open waters. Deep-water formation is very active in the northwestern Mediterranean Sea, where it influences intermediate and deep waters properties, nutrients replenishment and biological production. This study analyses, for the first time, the 20-year time series of monthly O_2 concentrations at the DYFAMED long-term sampling site in the Ligurian Sea. Until the winters of 2005 and 2006, a thick and strong oxygen minimum layer was present between 200 and 1300 m because dense water formation was then local, episodic and of low intensity. In 2005–2006, intense and rapid deep convection injected 24 mol O_2 m^{-2} between 350 and 2000 m from December 2005 to March 2006. Since this event, the deep layer has been mostly ventilated during winter time by newly formed deep water spreading from the Gulf of Lion 250 km to the west and by some local deep mixing in early 2010, 2012 and 2013. In the context of climate change, it is predicted that the intensity of deep convection will become weaker in the Mediterranean, which could potentially lead to hypoxia in intermediate and deep layers with substantial impact on marine ecosystems. With the exception of winters 2005 and 2006, the O_2 changes in surface waters followed a seasonal trend that reflected the balance between air-sea O_2 exchanges, changes in the depth of the mixed layer and phytoplankton net photosynthesis. We used the 20-year O_2 time series to estimate monthly and annual net community production. The latter was 7.1 mol C m^{-2} yr^{-1}, consistent with C-14 primary production determinations and sediment-trap carbon export fluxes at DYFAMED.

1. Introduction

The spatial and temporal scales of physical processes in the Mediterranean Sea are one order of magnitude smaller than those in the global ocean (Somot et al., 2006), and environmental changes in the Mediterranean can occur at relatively short time scales. For example, a rapid and extensive change in dense water formation occurred in the eastern Mediterranean (known as Eastern Mediterranean Transient, EMT) in the late 1980s (Klein et al., 1999; Lascaratos et al., 1999; Malanotte-Rizzoli et al., 1999), followed by a westward propagation of the temperature and salinity of the new water mass in 2004–2005 (Gasparini et al., 2005; Schroeder et al., 2010b). The arrival of the EMT signal in the Tyrrhenian and Ligurian Seas (Fig. 1) increased the salt content of the Levantine Intermediate Water in the Western Mediterranean (LIW, a water mass that flows from the Eastern into the Western Mediterranean at intermediate depths). The propagation of the EMT pre-conditioned the intermediate water by slowly increasing both its temperature and salinity (Schroeder et al., 2010b). Once the modified LIW reached the northwestern basin, the intermediate water was dense enough to increase the intensity of mixing triggered by the successive cold winters and the losses of heat fluxes and surface buoyancy. However, modeling studies (Herrmann et al., 2010; Somot et al., 2016) downplayed the influence of the EMT propagation, i.e. several weak deep convection events before the winter of 2005 could have caused an increase in the heat and salt content at intermediate depths in the northwestern basin and finally a more pronounced LIW. In winter 2005, intense deep convection was observed in the northwestern region (Gasparini et al., 2005; Schroeder et al., 2006). This event (called WMT for Western Mediterranean Transient) and the intense mixing localized in the Ligurian Sea in winter 2006 produced a large amount of warmer, saltier and denser water that propagated into the entire western basin, changing the original structure of the intermediate and deep waters

* Corresponding author.
E-mail address: coppola@obs-vlfr.fr (L. Coppola).

https://doi.org/10.1016/j.pocean.2018.03.001
Received 20 July 2017; Received in revised form 24 January 2018; Accepted 5 March 2018
Available online 07 March 2018
0079-6611/

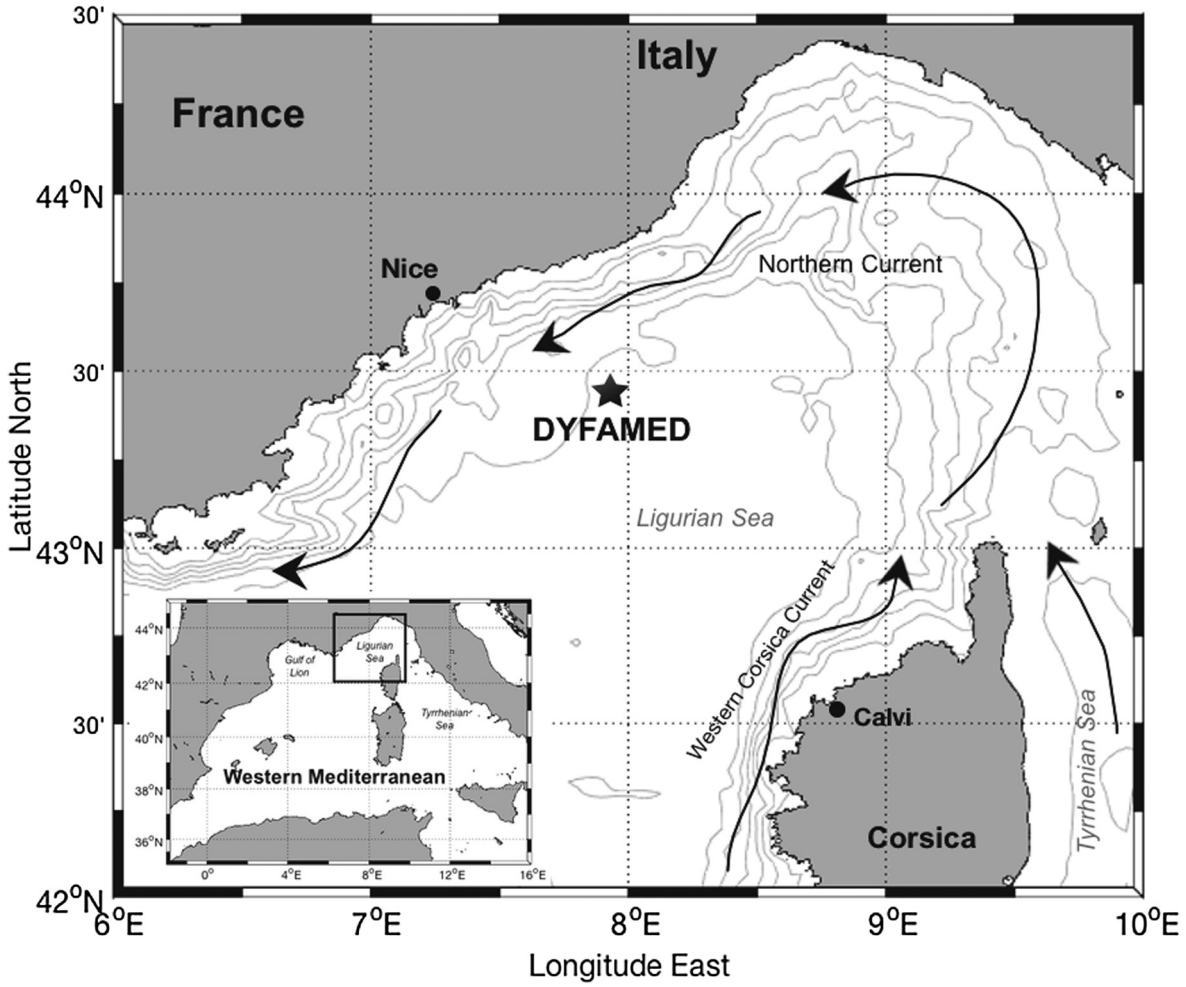

Fig. 1. Location of the DYFAMED site in the Ligurian Sea, Northwestern Mediterranean, with schematic representation of the main boundary current (Northern Current and Western Corsica Current, black arrow).

(Durrieu de Madron et al., 2013; Marty and Chiavérini, 2010; Schroeder et al., 2010b, 2008; Smith et al., 2008). The *in situ* observations in the western basin since year 2000 suggest that the succession of open-sea convection and shelf water cascading events caused a complete replacement of the resident deep water by a newly formed water mass (Schroeder et al., 2016, 2013). This rapid change influenced the oxygen and nutrient characteristics of the western intermediate and deep waters, but large uncertainties and the scarcity of observational data limit our understanding of the physical forcing on these biogeochemical variables (Schroeder et al., 2010a).

In the present study, we focus on O_2 variability in the northwestern Mediterranean Sea, which is well ventilated compared to the global ocean (Schneider et al., 2014). This ventilation can be deep enough to affect the intermediate and deep waters (Lascaratos et al., 1999; Roether et al., 1998; Roether and Schlitzer, 1991). Although the northwestern Mediterranean has limited exchanges with the global ocean, its rapid and active overturning circulation influences the Atlantic Ocean through the export of intermediate and deep waters, e.g. changes in T and S in the exported waters could affect the salinity and heat budget in the North Atlantic (Schroeder et al., 2016).

In the present work, we analyze the 20-year O_2 time series recorded at the DYFAMED site (water depth: 2347 m) located in the Ligurian Sea (Fig. 1). The DYFAMED oceanographic time series is one of the longest among the few existing oceanographic offshore time series in the Mediterranean Sea (Marty, 2002). Our objectives are to detect and interpret O_2 changes in the intermediate and deep-water masses (i.e. LIW and Western Mediterranean Deep Water, WMDW, respectively) during the two decades 1994–2014, estimate the photosynthetic production of O_2 in surface waters, and use the latter to obtain annual estimates of net community production.

2. Materials and methods

2.1. Study area and sampling methodology

The DYFAMED time series was initiated in 1991 within the framework of the Joint Global Ocean Flux Studies (JGOFS), at about the same time as the Bermuda Atlantic Time-Series Study (BATS) and the Hawaii Ocean Time Series (HOT) (Karl and Michaels, 1996), to monitor and investigate the physical, chemical and biogeochemical responses of the ocean to climate variability and anthropogenic inputs (Marty, 2002). The DYFAMED site is located in the central zone of the Ligurian Sea (43°25 N, 7°52E, Fig. 1), in the northwestern Mediterranean Sea, 30 nautical miles off the city of Nice. This site is outside the surface (Atlantic) water cyclonic boundary circulation and the underlying vein of LIW. This causes a doming of the isopycnals, at the top of which the DYFAMED site is located (Bethoux et al., 1982; Bethoux and Prieur, 1983).

This site is part of both the Ligurian node of EMSO (European Multidisciplinary Seafloor and water-column Observatory; http://www.emso-eu.org) and the French MOOSE (Mediterranean Ocean Observing System for the Environment; http://www.moose-network.fr).

In the present study, we used the post-calibrated CTD profiles

recorded monthly at the DYFAMED site from surface down to 2300 m (SBE 911plus) during the last 20 years (http://doi.org/10.17882/43749) (Coppola et al., 2016). The CTD sensors were calibrated every year. During CTD casts, seawater was sampled at 12 depths down to 2000 m with Niskin bottles mounted on a rosette: 10, 20, 30, 50 (i.e. near the deep chlorophyll maximum), 80, 100, 200, 400, 700, 1000, 1500 and 2000 m. Additionally, we compared the shipborne CTD profiles with the data from the mooring dataset deployed at DYFAMED since July 2009. This mooring has P, T and S sensors (SBE37 SMP) at different depths (200, 350, 700, 1000, 1500 and 2000 m), which acquire data every 6 min (Table S2). These sensors are maintained every year, and post-calibrated every second year, and they are compared with a dedicated CTD cast (sensors mounted on a CTD-rosette) during the yearly maintenance. To correct drift in the mooring dataset, we used the methodology described by Houpert et al. (2016). In this study, we compare the monthly shipborne CTD profiles with mooring sensors at the strategic depths of 350 m for the LIW and 2000 m for the WMDW. Because of a battery problem, the 350 m sensor stopped functioning from the end of 2010 to mid-2012. Hence the comparison between shipborne and mooring measurements at 350 m will only concern the period from mid-2012 to the end of 2014, whereas at 2000 m measurements will be compared from mid-2009 to the end of 2014.

2.2. Oxygen sampling and data processing

We analyzed the 182 T, S and O_2 profiles recorded during the period 1994–2014 (Table S1). All T and S data were post-calibrated (Seabird Application Note N°31, February 2010), and spikes and out of ranges data were removed prior to analysis.

Dissolved oxygen concentrations were systematically recorded together with T and S. They were measured with Seabird Clark electrode polarographic sensors (accuracy ± 2% of saturation): SBE13Y (theoretical accuracy 0.1 ml l^{-1}) from 1994 to 2002, and SBE43 (accuracy specified as 2% saturation, which is 0.12 ml l^{-1} for a solubility of 5.8 ml l^{-1} at 13 °C and salinity 38) from 2003 to 2014. During each monthly cruise, seawater samples from the 12 Niskin bottles were analyzed by Winkler titration (Winkler, 1888) to correct for possible O_2 sensor drift as recommended by Seabird (Janzen et al., 2007). As the drift effect on sensor calibration is not linear, it is strongly recommended to correct the sensor response by adjusting the sensor calibration coefficients with the Winkler-titrated water samples, considering the latter as the O_2 reference concentrations (Uchida et al., 2010). Following this recommendation, we matched the up-cast profiles data to the up-cast water samples data based on pressure, and minimized the residual of the squared differences between the calibrated and water sample O_2 data by adjusting the calibration coefficients. To ensure high robustness of the data adjustment, we maximized the number of samples used to determine each set of coefficients by using the largest possible number of consecutive profiles (i.e. samples with a constant O_2 drift). We finally re-processed the O_2 down-cast profiles using the new adjusted SBE13/SBE43 calibration coefficients (Fig. S1).

2.3. Estimation of mixed layer depth

To estimate the strength of the mixing process on O_2 variations, we use the mixed layer depth (MLD), which indicates the depth reached by turbulent mixing in a recent past. We calculated the MLD as the depth where the difference of density from the surface reference (i.e. density at 10 m depth) was 0.03 kg m^{-3} (D'Ortenzio et al., 2005; de Boyer Montégut, 2004). The density profiles had been calculated from T and S profiles, and linearly interpolated at 1 m depth intervals. When no density value was available at 10 m, the shallowest available value was used as the surface reference if it was < 20 m, otherwise the MLD was not computed for that date (Pasqueron de Fommervault et al., 2015). We also calculated the T, S and O_2 average values in the mixed layer based on the approach of Nilsen and Falck (2006), i.e. we integrated T, S and O_2 vertically (trapezoidal method) over the mixed layer and divided the result by the MLD (T_{MLD}, S_{MLD} and DO_{MLD}).

2.4. Estimation of net community production

The upper ocean can be divided in two zones that are reflected in the O_2 dynamics. The production zone is located between the surface and the compensation depth, which is the depth where the difference between gross primary production and total community respiration (called Net Community Production, NCP) is equal to zero. This zone is the site of air-sea gas exchange, photosynthesis and respiration. The consumption zone is located below the compensation depth (i.e. usually below 100 m), and is dominated by respiration processes (Cianca et al., 2013). The NCP can be expressed in units of either oxygen or carbon. Positive NCP is considered to indicate net autotrophy (i.e. net *in situ* production of organic carbon), whereas negative NCP is considered to indicate net heterotrophy (i.e. net consumption of organic carbon). In the present paper, we estimated NCP in the production zone from the O_2 excess above 100% saturation (ΔO_2 in mol O_2 m^{-2}) (Emerson and Bushinsky, 2014; Emerson et al., 1995; Jenkins and Goldman, 1985; Najjar and Keeling, 1997; Riser and Johnson, 2008). The depth of 100% O_2 saturation corresponds in practice to the compensation depth. We estimated the value of ΔO_2 as the O_2 inventory from the surface down to the 100% saturation depth, assuming that the O_2 saturation isopleth (where O_2 saturation = 100%) separated the production and consumption zones (Cianca et al., 2013).

We estimated the net amount of O_2 produced during one year (O_2 Prod) as the difference between the maximum and minimum ΔO_2 during the year (ΔO_{2max} and ΔO_{2min}, respectively) divided by the number of days between the two values (Δt, days), and extrapolated to the whole year by multiplying by 365 d yr^{-1}:

$$O_2\ \text{Prod}\ [\text{mol}\ m^{-2}\ yr^{-1}] = (\Delta O_{2max} - \Delta O_{2min}) \times (365)/\Delta t \quad (1)$$

The net annual O_2 production (Eq. (1)) combines two processes, i.e. the annual NCP (expressed in O_2 units) and the upward and downward O_2 fluxes based on the net air-sea exchange in the production layer (FO_2):

$$O_2\ \text{Prod} = \text{NCP (oxygen)} + FO_2 \quad (2)$$

We used the following equation to determine the air-sea exchange flux:

$$FO_2\ [\text{mol}\ m^{-2}\ yr^{-1}] = k_{O2} \times (O_{2sat} - O_{2sw}) \quad (3)$$

where k_{O2} (m s^{-1}) is the exchange coefficient for O_2, O_{2sat} is the 100% oxygen saturation when water is equilibrated with air, and O_{2sw} is the oxygen concentration in surface water (Copin-Montégut and Bégovic, 2002). To estimate k_{O2}, we used the wind-speed parameterization of Ho et al. (2006), which is based on a quadratic relationship between wind speed and gas transfer velocity:

$$k_{O2}\ [\text{m}\ d^{-1}] = 0.266 \times u^2 \times (Sc/660)^{0.5} \times 24/100 \quad (4)$$

where u is the average wind speed, and Sc the Schmidt number for O_2 (kinematic viscosity of water, divided by diffusion coefficient of the gas in water).

Finally, we calculated the annual NCP using the estimates of net annual O_2 production and the net air-sea O_2 flux (Eqs. (1)–(3)):

$$\text{NCP (oxygen)} = O_2\ \text{Prod} - FO_2 \quad (5)$$

We obtained the NCP in term of carbon using the Redfield et al. (1963) ratio of O_2:C = 138:106 = 1.3:

$$\text{NCP (carbon)} = \text{NCP (oxygen)}/1.3 \quad (6)$$

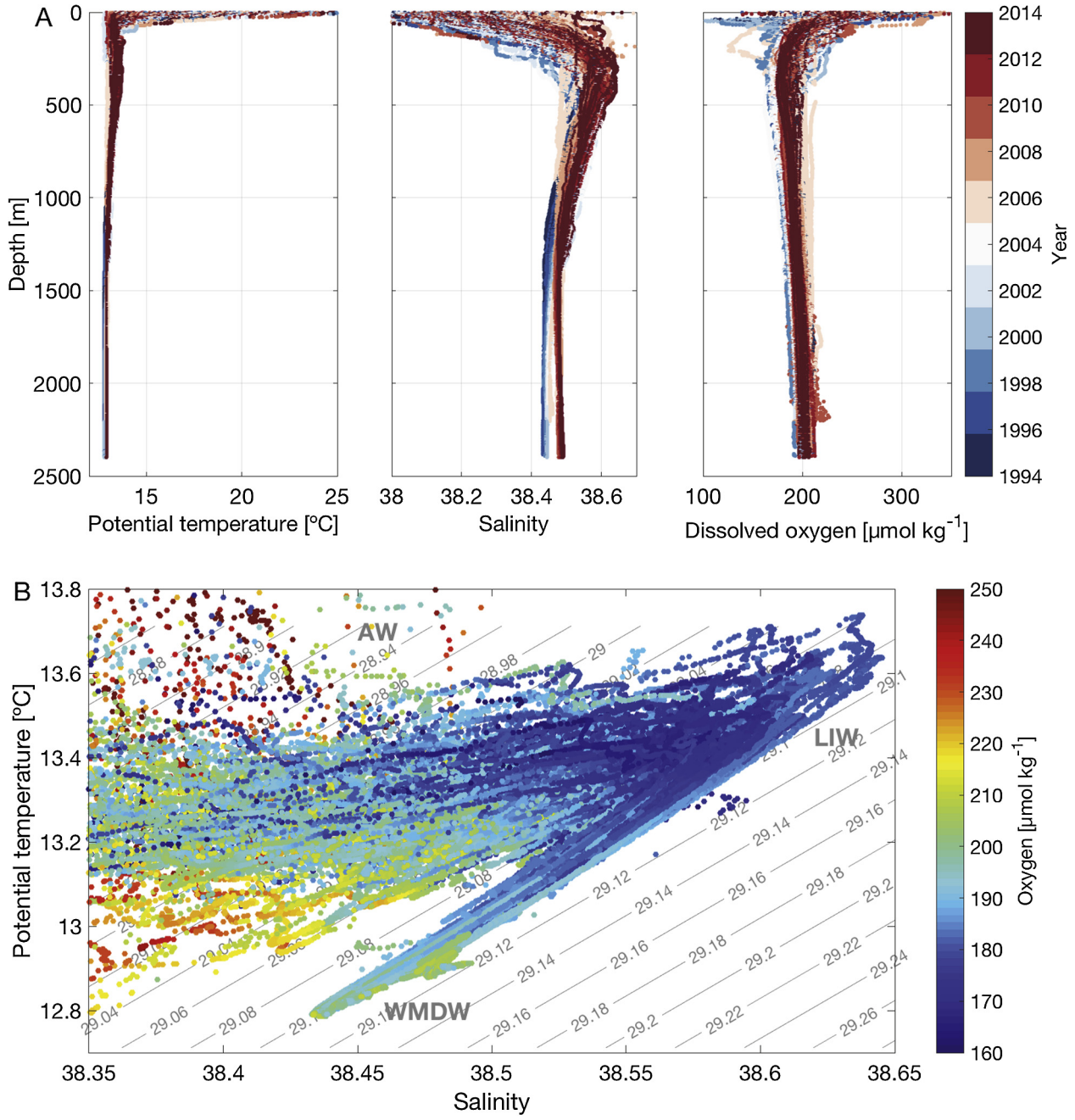

Fig. 2. DYFAMED time series 1994–2004. (A) Combined vertical profiles of Θ, S and dissolved O_2 for the whole time series. The different colors correspond to the years of profiles. (B) Θ-S diagram with the positions of three water masses defined in the text: AW, LIW and WMDW. The colors of dots represent the concentrations of dissolved O_2. (For interpretation of the references to colour in this figure legend, the reader is referred to the web version of this article.)

3. Results

3.1. Hydrological characteristics

The combined vertical profiles of potential temperature (Θ), S, and O_2 from 1994 to 2014 show that the interannual and seasonal variability of the three variables decreased with depth (Fig. 2A). Variability was largest in the upper 200 m (13.3–25 °C, 37–38.6, and 80–350 µmol kg^{-1} for Θ, S, and O_2, respectively), and smallest below 600 m (13–13.2 °C, 38.4–38.5, and 200–210 µmol kg^{-1}, respectively). The "scorpion–tail" shape of the Θ–S diagram (Fig. 2B) reflects coincident subsurface Θ and S maxima, which are represented in the upper right-hand corner of the diagram. Three main water masses can be identified on the Θ–S diagram: Atlantic Water (AW) in the upper 200 m (Θ = 12.8–25 °C, S = 37.5–38.5) with variable O_2 concentrations, LIW between 200 and 600 m (Θ = 13.2–13.5 °C, S = 38.5–38.6) with high S and O_2 concentrations between 160 and 180 µmol kg^{-1}, and WMDW below 600 m (Θ = 12.8–12.9 °C, S = 38.4–38.5) with higher O_2 concentrations than the LIW.

The depths of the Θ, S and O_2 isopleths showed strong seasonal variations and some inter-annual changes between 1994 and 2014 (Fig. 3). Year after year, there were successive periods of winter mixing and summer stratification in the three variables. The highest S and minimum O_2 concentrations in the whole data series (S = 38.56–38.64 and O_2 = 160–185 µmol kg^{-1}, respectively), associated with relatively high Θ (13.5–13.7 °C), occurred between 200 and 600 m, near the core of the LIW.

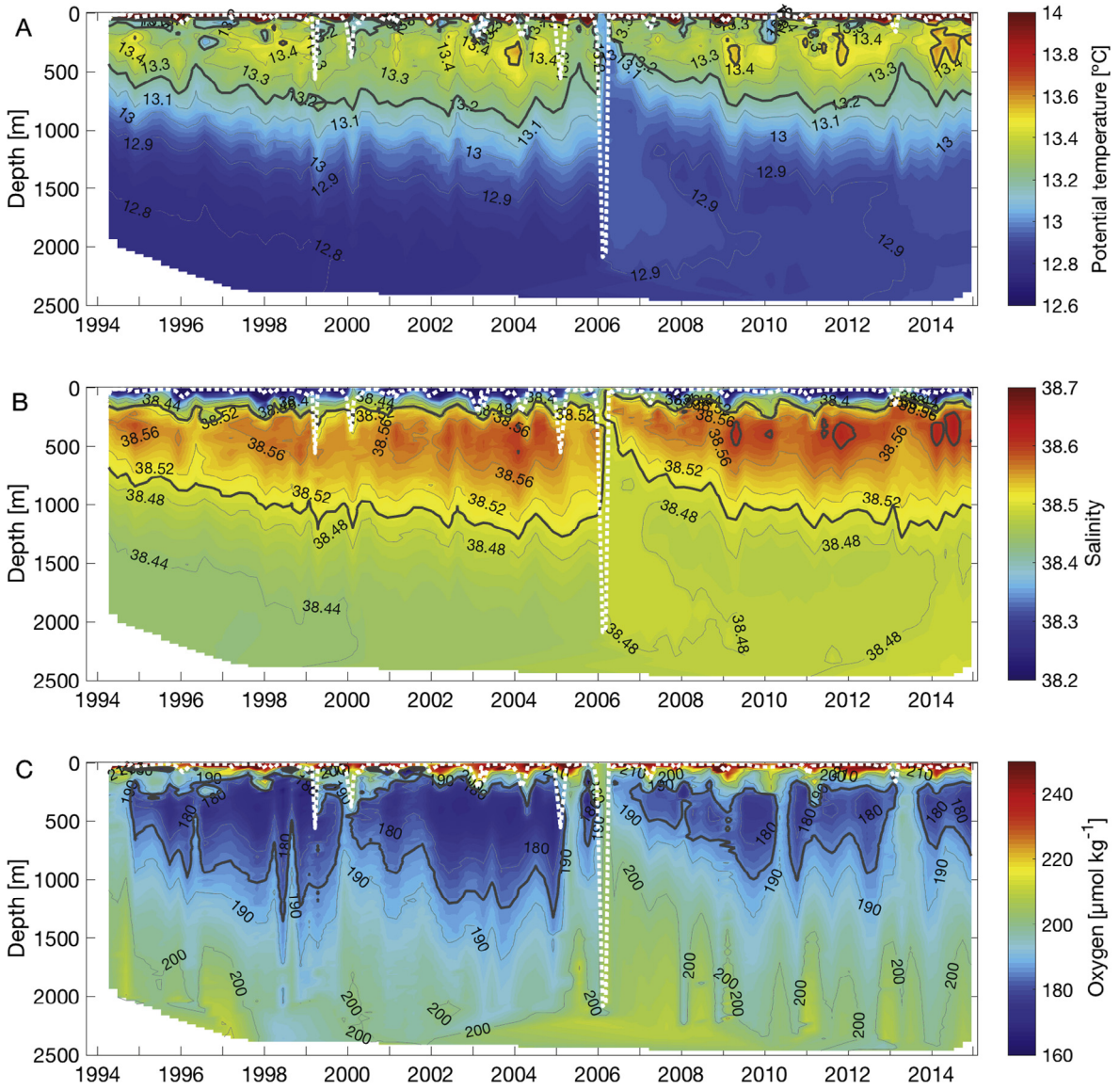

Fig. 3. Temporal variations in the depths of isopleths from surface to bottom at DYFAMED from 1994 to 2014: (A) Θ, (B) S, and (C) dissolved O_2. White dashed line: MLD estimated from the potential density threshold of 0.03 kg m^{-3}. (A) and (B) Dark lines: deep and shallow limits of the LIW, at Θ = 13.2 and 13.5 °C and S = 38.5–38.6, respectively. (C) Dark lines: deep and shallow limits of the O_2 minimum layer, at 185 µmol O_2 kg^{-1}.

3.2. Oxygen minimum layer and WMDW characteristics

The Oxygen Minimum Layer (OML) at DYFAMED is located between the isopleths of 185 µmol kg^{-1}, from about 200 to 1300 m (Fig. 3C). Its minimum values during the period 1994–2014 were 160 µmol kg^{-1}. The OML was located at intermediate depths from 1994 to 1999 and 2000 to 2005. After 2006, the thickness of the OML decreased and its lowest O_2 concentrations were > 170 µmol kg^{-1}, with strong seasonal and interannual variability in both thickness and lowest O_2 concentrations until the end of the reported observation period in 2014.

The depth of minimum O_2 concentration (z_{O2min}) was deeper than that of maximum Θ but close to that of maximum S (mean depths of 363 m compared to 311 and 368 m, respectively; Fig. S2A and S2B). Both Θ and S at z_{O2min} in the OML showed strong seasonal variations and they increased by 0.15 °C and 0.05, respectively, from 2000 to 2005 (Fig. 4A and B). Mean Θ and S at z_{O2min} showed a first decrease at the end of 2004 and in early 2005 and a second rapid drop at the end of 2005 and in early 2006 (by 0.4 °C and 0.07, respectively), after which they increased continuously until (by 0.3 °C and 0.08 over the last 6 years of the series, respectively) until early 2013 when a rapid decrease of Θ and S was observed (by 0.2 °C and 0.05, respectively). The trend of the monthly shipborne Θ and S data was consistent with those from the mooring at 350 m from mid-2012 to the end of 2014. However, high frequency measurements from the mooring at 350 m showed a short event of Θ and S mixing in the end of 2012 and a rapid decrease in February-March 2013. After these events, the two datasets showed a continuous increase of Θ and S until the end of the reported observation period in December 2014 (by 0.3 °C and 0.1, respectively).

Temporal variations in minimum O_2 concentrations (Fig. 4C) showed the following changes from 1999 to 2014: a decrease of 7 µmol kg^{-1} yr^{-1} from April 1994 to March 1999; rapid increases from 155 to 180 and from 170 to 190 µmol kg^{-1} in winter 1999 and in winter 2000, respectively; a second decrease of 4 µmol kg^{-1} yr^{-1} from March 2000 to November 2005; a second set of rapid increases from 160 to 190 and from 150 to 200 µmolO_2 kg^{-1} in March 2005 and February 2006, respectively; and relatively constant values after March 2006 (average of 180 µmolO_2 kg^{-1} between 2006 and 2014) except during the winter 2012–2013 when minimum O_2 concentrations increased to 190 µmol kg^{-1}. The five rapid increases in minimum O_2

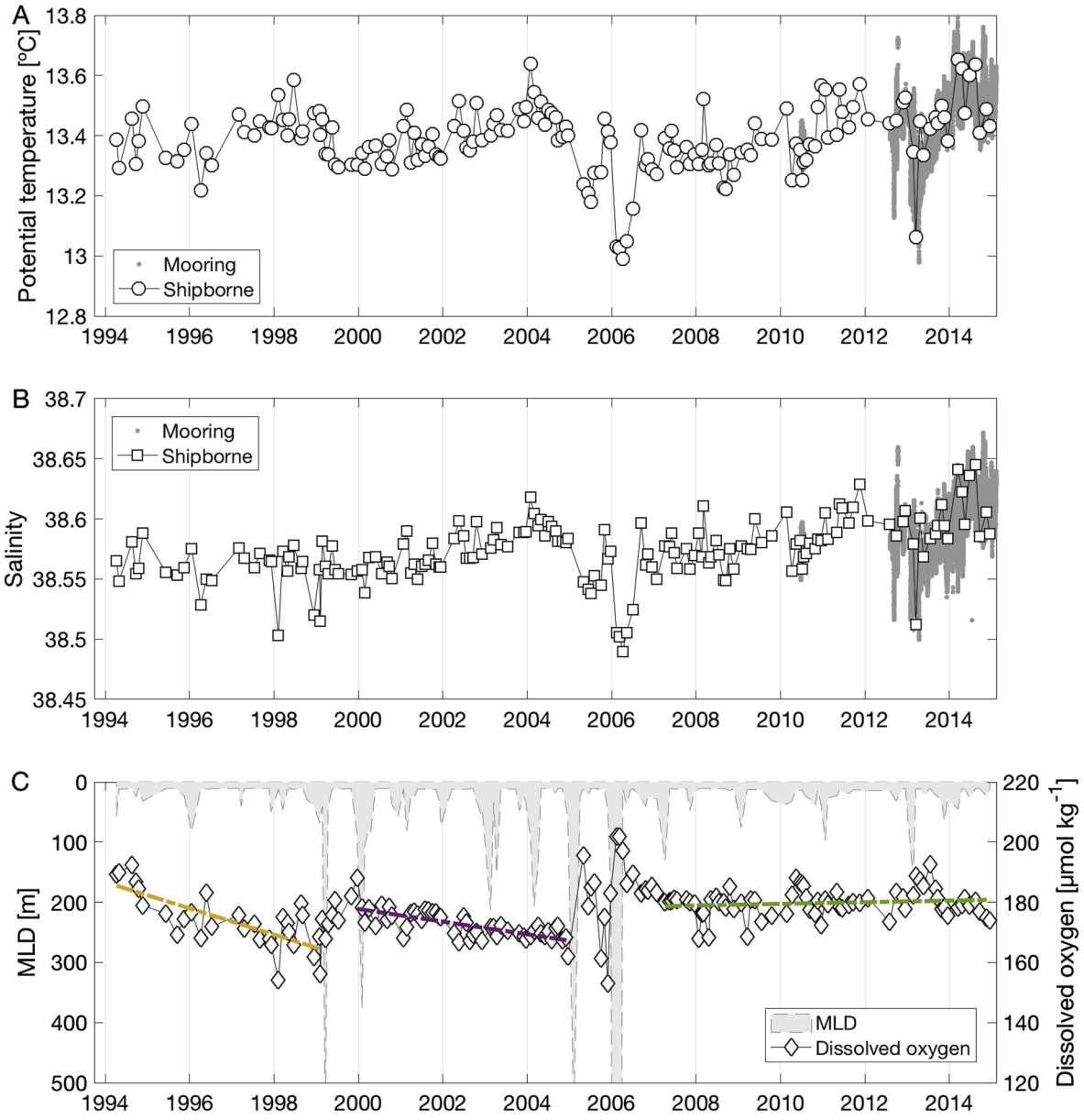

Fig. 4. Temporal variations at DYFAMED in 1994–2014: (A) Θ from monthly shipborne profiles (grey circles and solid line) at z_{O2min}, and from a mooring at 350 m (grey dots). (B) S from monthly shipborne profiles (open squares and dashed-dot line) at z_{O2min} and from mooring at 350 m (grey dots, 2012–2014). (C) MLD (left axis, grey area) and minimum O_2 concentration at z_{O2min} (right axis, open diamonds and line). Three dashed lines (colored): linear regressions of minimum O_2 at z_{O2min} on time (months) during three periods, i.e. 1994–1999 (yellow), 2000–2004 (purple), and 2006–2014 (green). (For interpretation of the references to colour in this figure legend, the reader is referred to the web version of this article.)

concentrations (i.e. February-March 1999, January-February 2000, February-March 2005, February-March 2006, and February-March 2013) corresponded to sharp increases in the MLD (Fig. 4C).

At 2000 m in the WDMW, there was a slow increase in Θ and S from 1994 to 2005 ($+0.005\,^{\circ}C\,yr^{-1}$ and $+0.0022\,yr^{-1}$, respectively) and a slow decrease in O_2 concentration from 1995 to 2004 ($10\,\mu mol\,kg^{-1}\,yr^{-1}$; Fig. 5A, 5B and 5C). After the winters 2004–2005–2006, there was a rapid increase in Θ, S and O_2 ($+0.1\,^{\circ}C$, $+0.03$ and $+15\,\mu mol\,kg^{-1}$, respectively; Fig. 5A–C), followed by slow decreases in Θ and S from 2006 to 2011, after which the two variables started to increase as they had done before the 2004–2005–2006 event. However, high frequency observations from the mooring at 2000 m showed fast increases in Θ and S in early 2010, 2012 and 2013 that had not been observed in the monthly shipborne monitoring ($< 0.05\,^{\circ}C$ and < 0.01, respectively; Fig. 5A and B). No trend could be identified in O_2 at 2000 m after 2007 because of the strong monthly variability in this variable (Fig. 5C). From 2006 onwards, the WMDW was characterized by Θ = 12.88–12.92 °C, S = 38.48–38.49 and O_2 = 195–210 $\mu mol\,kg^{-1}$.

The very rapid increases in Θ, S and O_2 concentrations in deep waters between December 2005 and February-March-April 2006 are detailed in Fig. 6. The O_2 content between 350 m (the mean LIW depth) and 2000 m were 324, 344, 348 and 339 $mol\,m^{-2}$, in December 2005, and February, March and April 2006, respectively. It follows that 24 $mol\,m^{-2}$ of O_2 were injected between 350 and 2000 m from December 2005 to March 2006, and 9 $mol\,m^{-2}$ were lost in the following month, the average rates of O_2 injection and loss being both about 0.3 $mol\,m^{-2}\,d^{-1}$.

O_2 concentrations plotted on the Θ-S diagrams show that Θ, S and O_2 concentrations in deep waters were constant from 1996 to 2004 and slightly higher in O_2 in 1994 (Fig. 7). From 2005 to 2006, the deep waters showed very high O_2 concentrations associated with an increased Θ and S, creating a “hook” in the Θ-S diagrams that persisted until 2010. After 2010, the hook was reduced, but the bottom water continued to show high salinities and O_2 concentrations.

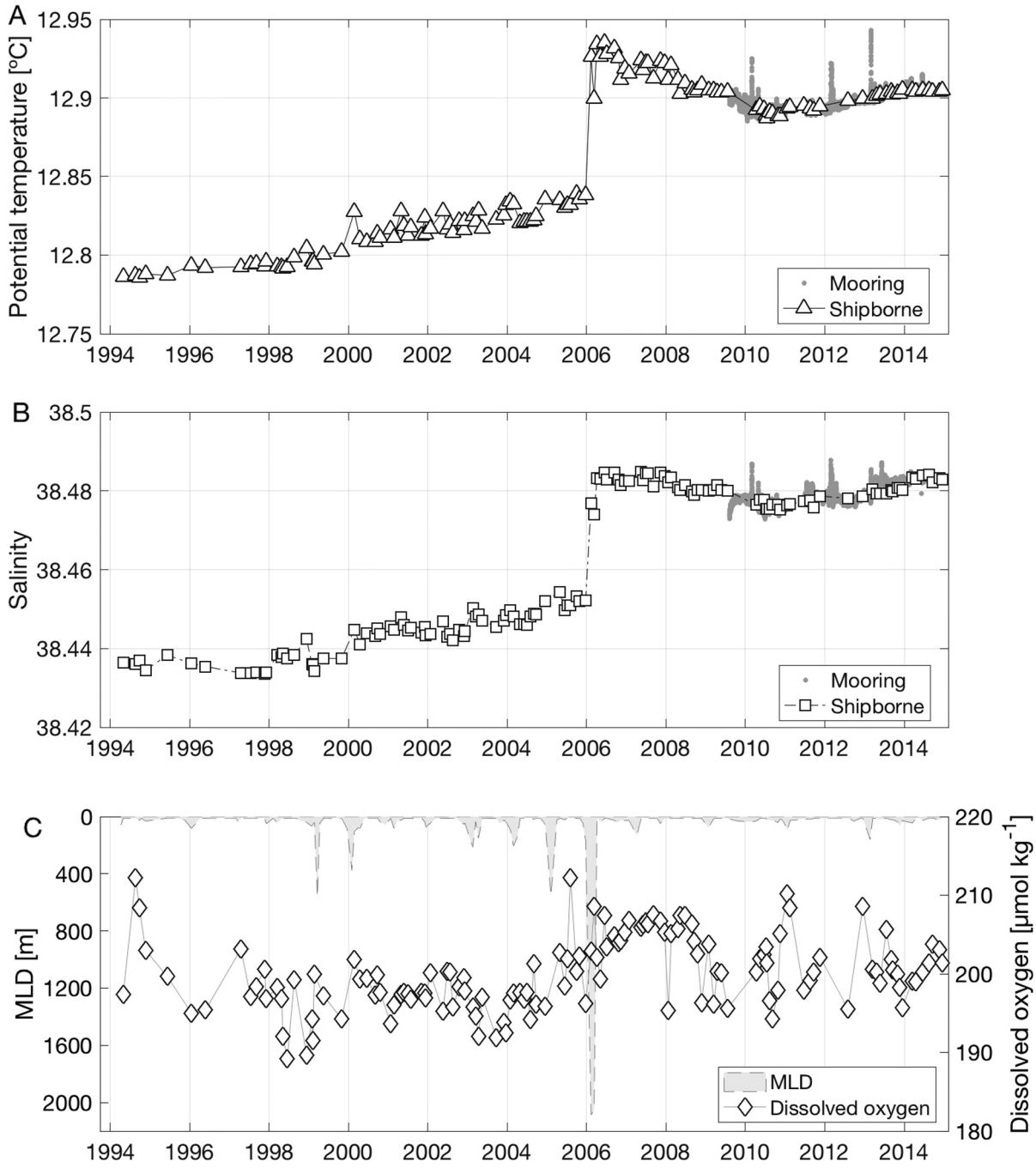

Fig. 5. Time series at 2000 m at DYFAMED in 1994–2014: (A) Θ from monthly shipborne profiles (open triangles, solid line) and from a mooring (grey dots, 2009–2014). (B) S from monthly shipborne profiles (open squares, dashed-dot line) and from the mooring (grey dots, 2009–2014). (C) MLD (left axis, dashed line) and dissolved O_2 concentration (open diamonds, solid line).

3.3. Seasonal variability of oxygen in the mixed layer

The 1994–2014 average seasonal cycles were not the same for mean MLD, T_{MLD}, S_{MLD} and DO_{MLD} (not including the extreme values of winter 2005–2006) (Fig. 8). *In situ* temperature was used here instead of Θ to describe the influence of the variability of the mixed layer without including effects of salinity, which is involved in the calculation of Θ. The mean MLD values ranged between 50 and 80 m in winter (December-March) and 10–15 m in summer (May to September). The mean T_{MLD} ranged between 13.5 and 14.5 °C in winter (minimum in February) and 16.5–22.5 °C in summer (maximum in August). The seasonal variability of the mean S_{MLD} was very small, with values ranging from 38.02 (May and November) to 38.25 (August). The pattern of variation of mean DO_{MLD} was very different from that of mean T_{MLD} and S_{MLD}, i.e. an increase from February through April, minimum values from July through October, and slightly higher values from November through February.

3.4. Net community production

The mean potential density in surface waters was highest in winter and lowest in summer (Fig. S3A). The mean saturation isopleth (i.e. depth at which the O_2 is at 100% saturation), which defines the lower limit of the production layer, was around 40 m from April to October, near 80 m in November-December, and close to surface from January to March (Fig. S3B). In the production layer, the annual cycle of ΔO_2 was

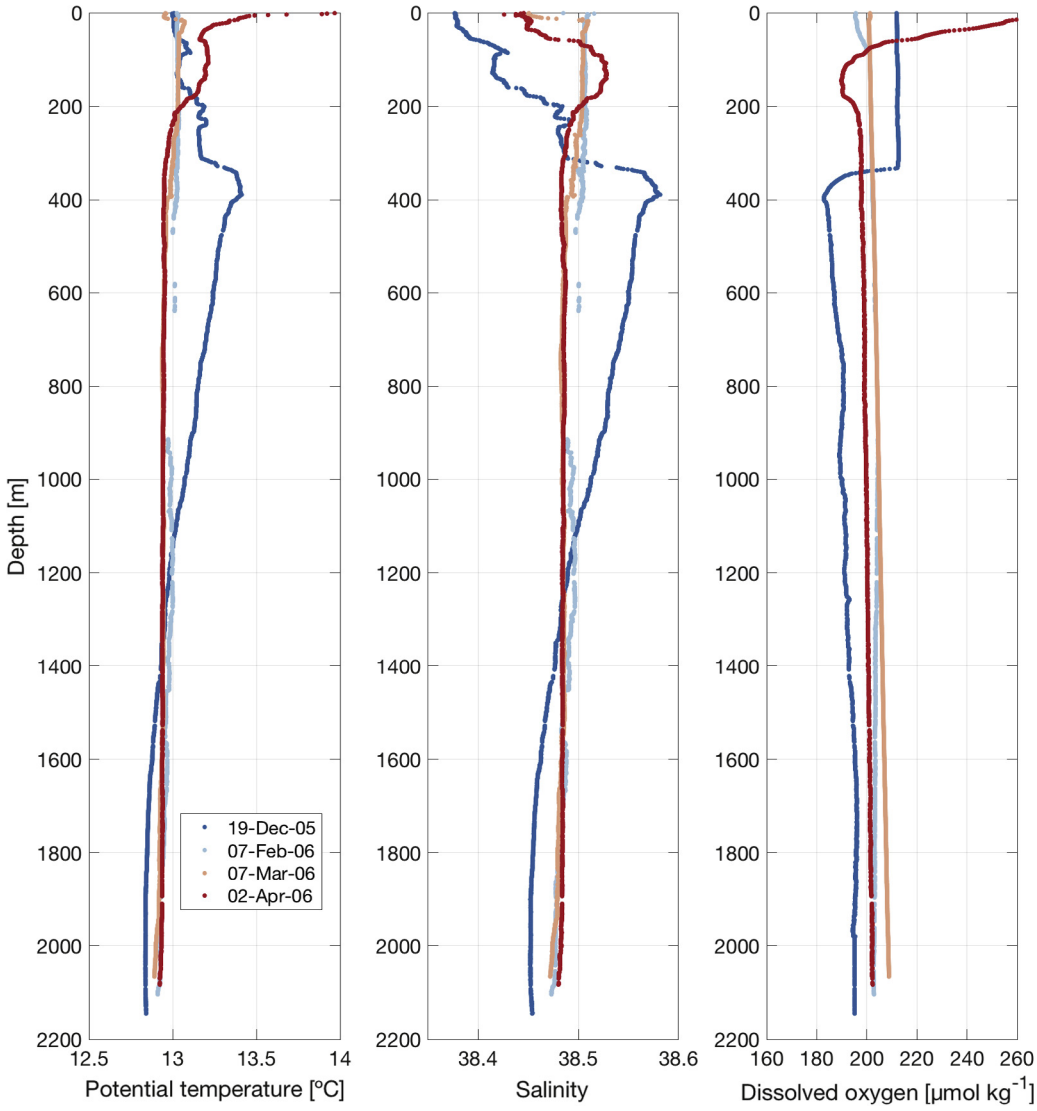

Fig. 6. Vertical profiles of Θ, S, and dissolved O_2 at DYFAMED in December 2005 (blue dots), February 2006 (clear blue dots), March 2006 (clear red dots) and April 2006 (red dots). (For interpretation of the references to colour in this figure legend, the reader is referred to the web version of this article.)

characterized by a minimum in winter (from mid-December to the end of January) and a maximum in spring/early summer (from mid-April to mid-July) (Fig. 9). Based on the seasonal variation of ΔO_2 in the production layer, the net annual O_2 production was O_2 Prod = 6.6 ± 1.7 mol O_2 m^{-2} yr^{-1} (Eq. (1)).

Calculation of the NCP (oxygen) (Eq. (5)) requires estimating the air-sea exchange flux in the upper 40 m (which is the maximum value of the saturation isopleth), which we calculated using Eq. (3). The latter equation includes k_{O2}, whose calculation requires knowing the wind speed (Eq. (4)). At DYFAMED, the annual mean wind speed computed from values recorded hourly by a meteorological buoy since 1999 (ODAS Côte d'Azur, Météo France) ranged from 0.9 to 9.2 m s^{-1} (mean of 5.2 ± 1.2 m s^{-1}), giving k_{O2} = 1.8 ± 0.1 m d^{-1} (Eq. (3)). This value is lower than the k_{O2} estimated by Copin-Montégut and Bégovic (2002), but the latter value had been based on two winter months, during which wind speed was high, whereas our k_{O2} estimate is based on observations made over 20 years. Our monthly estimates of the air-sea O_2 flux ranged between FO_2 = −15.1 to 14.8 molO_2 m^{-2} yr^{-1} (mean of −2.6 molO_2 m^{-2} yr^{-1}), with positive values (net ingassing) from December to March when wind speed and O_2 solubility (low surface temperature) were higher, and negative values (net outgassing) from April to November when surface water was saturated in O_2 and the O_2 from photosynthesis escaped to the atmosphere (Fig. S4). The resulting annual mean NCP (oxygen) was 9.2 molO_2 m^{-2} yr^{-1} (Eq. (5)). This corresponds to NCP (carbon) = 7.1 molC m^{-2} yr^{-1} or 85.2 gC m^{-2} yr^{-1} (Eq. (6)).

4. Discussion

4.1. Interannual variability of the OML

The LIW is the warmest and saltiest water at depth in the western Mediterranean basin, with maximum Θ and S above and below the LIW core, respectively (Millot and Taupier-Letage, 2005). It was suggested that, in the western Mediterranean, the OML approximately coincides with the mean depth of the LIW, which is located at 300–400 m (Tanhua et al., 2013). In the Mediterranean Sea, the OML corresponds to the lowest O_2 concentrations where O_2 consumption (fueled by organic matter inputs) exceeds the O_2 replenishment via the processes of advection and diffusion (Packard et al., 1988; Tanhua et al., 2013). Comparing the depths of the Θ and S maxima with the depth of the O_2 minimum at DYFAMED indicates that the vertical position of the OML may be close to that of the S maximum (mean values of 360 and 370 m, respectively), which corresponds to the core of the LIW (Figs. S2A and S2B).

The presence of the OML is generally explained by the fact that the

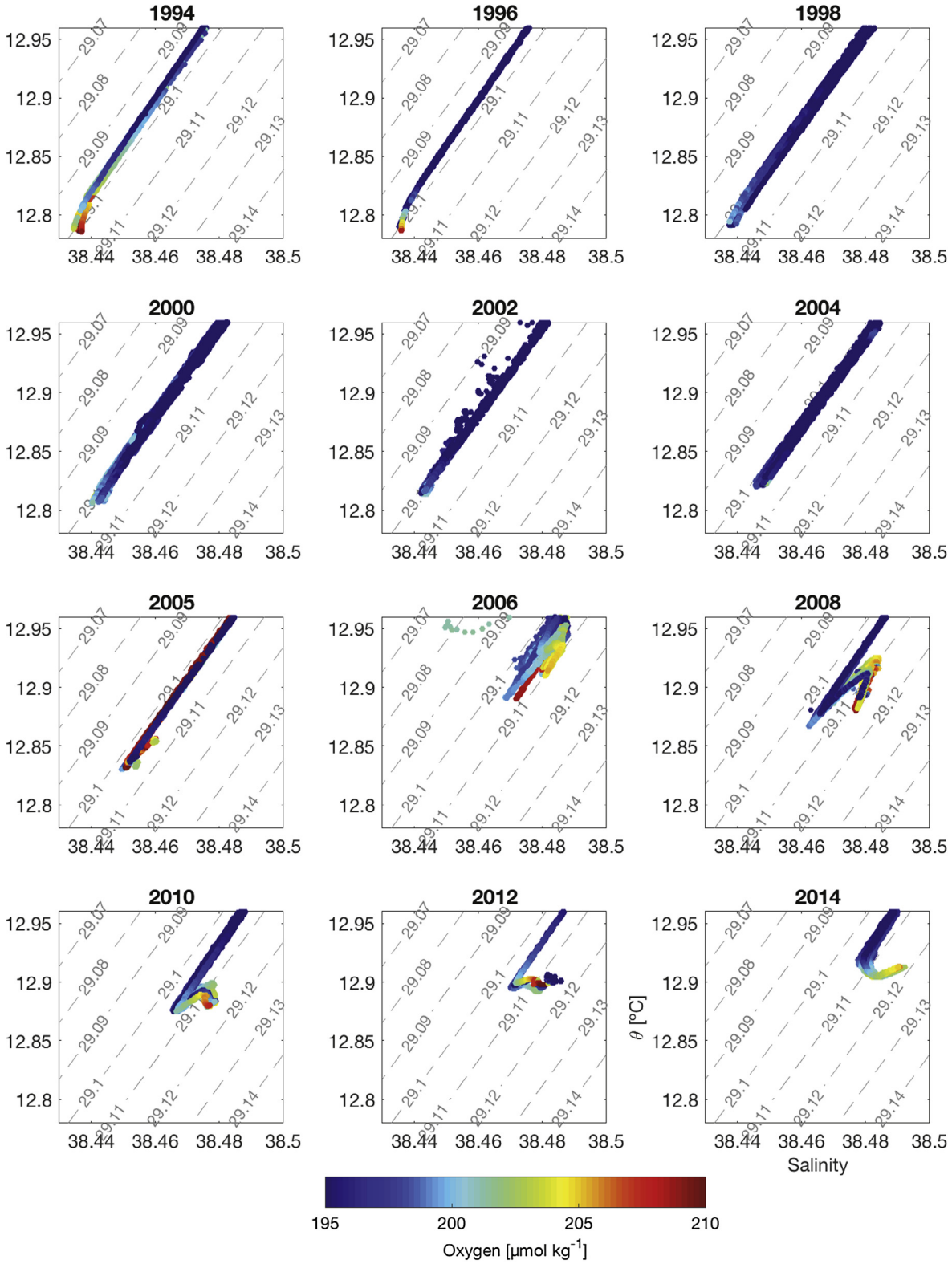

Fig. 7. Θ-S diagrams of data below 2000 m at DYFAMED in 1994–2014. The different colors correspond to different O_2 concentrations. Grey Dashed grey lines: isopycnals. (For interpretation of the references to colour in this figure legend, the reader is referred to the web version of this article.)

LIW contains the oldest waters in the western Mediterranean Sea (Millot and Taupier-Letage, 2005). Indeed, the local oxygen concentration and the depth of the OML reflect the balance between the supply and consumption of O_2 since the formation of the LIW in the eastern Mediterranean. During the transit of the LIW from the eastern to the western Mediterranean, the consumption of organic matter coming from the surface progressively creates a O_2 minimum in the water mass. The characteristics of the O_2 minimum also depends on the vertical mixing events that occurred during the east-west transit (e.g. formation of deep water) and the mixing through advective processes. The OML is maintained near the LIW because biological O_2 utilization there exceeds the rate of O_2 replenishment via physical processes. This is consistent

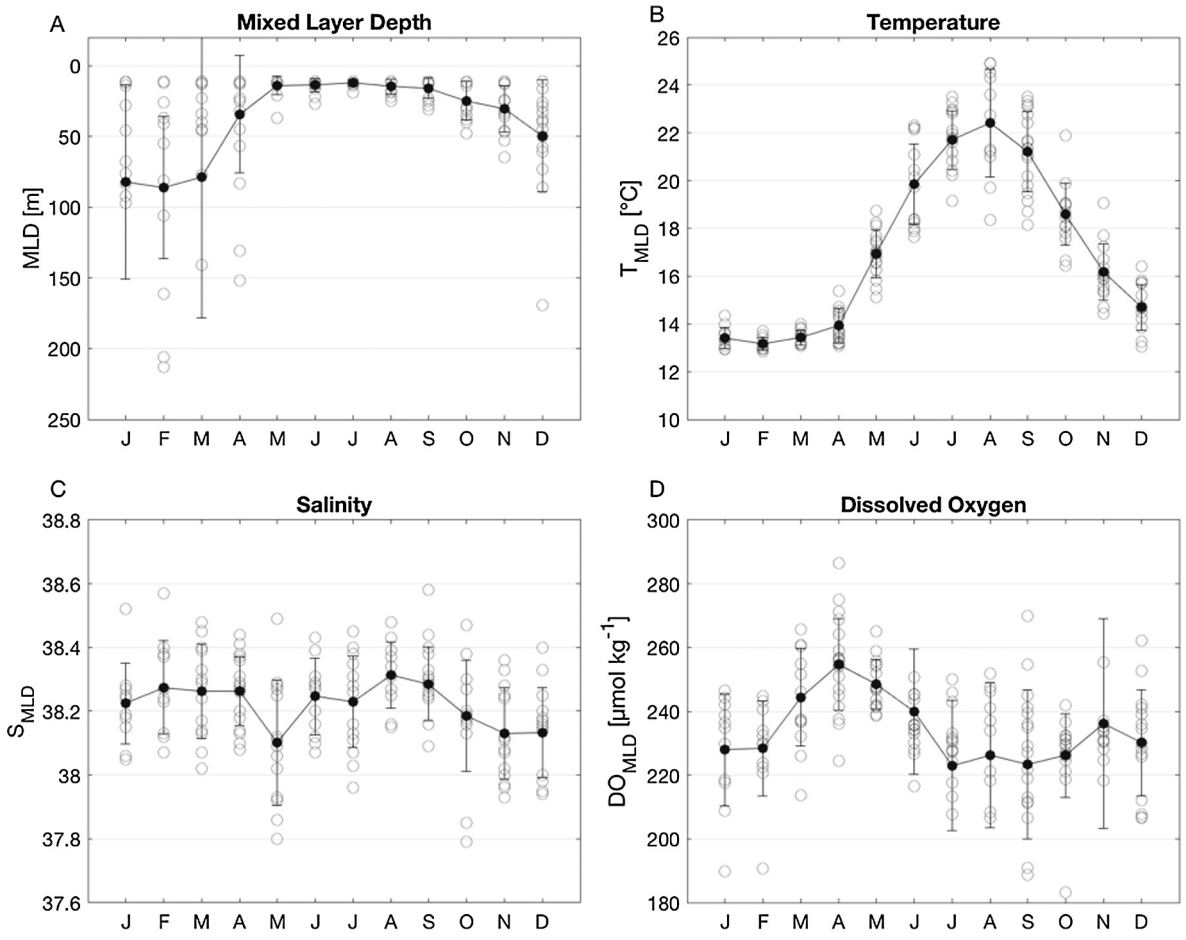

Fig. 8. Monthly variations at DYFAMED in 1994–2014 (not including the anomalous winter 2005–2006) of (A) MLD, (B) T_{MLD}, (C) S_{MLD}, and (D) DO_{MLD}. In each panel, the open dots are the individual observations, the black dots linked by a line are the annual mean values, and the vertical bars represent one standard deviation.

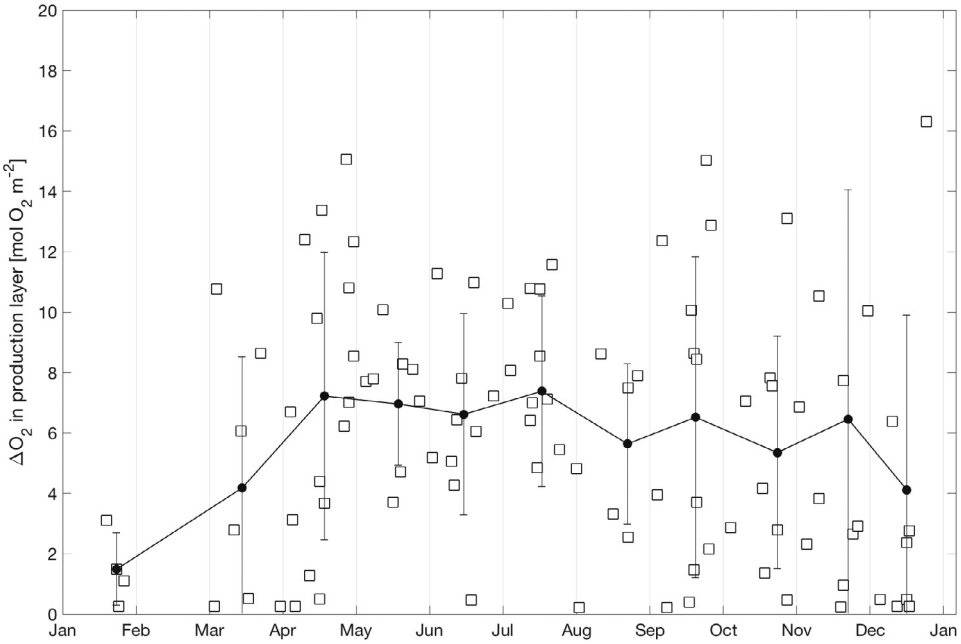

Fig. 9. Monthly variations in mean ΔO_2 in the production layer (i.e. waters above the black line in Fig. S3B) at DYFAMED in 1994–2014. The open squares are individual monthly values, the black dots linked by a line are monthly averages, and the vertical bars represent one standard deviation.

with the fact that in the Mediterranean Sea, high rates of organic matter remineralization are observed in intermediate and deep waters related to the downward export of dissolved organic carbon (DOC) (Lefevre et al., 1996), in particular during the period of winter deep-water formation (Copin-Montégut and Avril, 1993).

The OML at the DYFAMED site was located between 200 and 1300 m from 1994 to 2014 (Fig. 3C). The continuous presence of the OML was likely related to the absence of deep mixing during most winters in the Ligurian Sea, where deep convection events occurred only episodically (Estournel et al., 2016). Indeed, during the period 1994–2014, the MLD rarely exceeded 350 m, and there were only five main deep-mixing events (i.e. below the LIW), in February-March 1999, January-February 2000, February-March 2005, February-March 2006 and February-March 2013 (Fig. 4A and B). Even if the monthly sampling frequency at DYFAMED did not allow the observation of short-time-scale variations of the MLD, it is unlikely that mixing events shorter than one month would have injected large amounts of O_2 into the OML from the surface or deep waters. Consequently, the low intensity and deepening of vertical mixing at DYFAMED strengthened the signature of the OML. Moreover, remineralization processes, associated with downward inputs of DOC and sinking of organic particles, and low oxygen diffusion/advection were likely responsible for the maintenance of the strong and almost permanent OML (Figs. 3C and 4C), whereas recurrent and intense deep winter mixing more to the west, in the Gulf of Lion (Fig. 1), may have affected the signature of the OML (Durrieu de Madron et al., 2013; Houpert et al., 2016).

From 1994 onwards, two successive decreases in O_2 concentrations from 1994 to 1999 and from 2000 to 2005 showed intensification of the OML (Fig. 4C). This trend of OML intensification was interrupted twice by strong water-column mixing below 350 m in February-March 1999 and January-February 2000, which injected at depth O_2-rich surface water (Copin-Montégut and Bégovic, 2002). No such events were observed after the intense deep mixing of winters 2004–2005 and 2005–2006 (Borghini et al., 2014; Marty and Chiavérini, 2010; Smith et al., 2008).

The two successive decreases in O_2 in the OML can be explained by lateral inputs of O_2-poor surrounding waters and/or be the result of progressive consumption of O_2 by bacteria in the OML over several years. Concerning potential lateral inputs, isopycnal advection of the core of the LIW to the central zone of the Ligurian Sea (where DYFAMED is located) could have influenced the decrease in O_2 concentrations. Indeed, the core of the LIW, which is characterized by high T and S values and low O_2 concentrations, is located at the periphery of the central Ligurian Sea and affected by the Northern Current and the Western Corsica Current (Fig. 1; Bosse et al., 2015). In winter, the LIW outflow develops instabilities that increase the exchange between coastal and offshore regions (Prieur et al., 1983). In early spring, the vertical stratification and horizontal spreading is dominated by baroclinic instabilities developing at the periphery of the mixed patch (zone where intense vertical velocities are observed during winter convection) and is accompanied by increased coastal-offshore exchanges (Estournel et al., 2016). After the spring, isopycnal diffusion can slowly decrease the T, S and O_2 differences between the coastal and offshore zones.

Concerning bacterial respiration, the annual sinking flux of particulate organic carbon at 200 m has not substantially changed over time at DYFAMED since 1994 (Miquel et al., 2011), and the observed decreases in O_2 concentrations could be explained by the cumulative effect of steady bacterial O_2 consumption over time. Consequently, the periods of OML intensification probably resulted from a combination of the absence of strong vertical mixing in winter during the 1994–1999 and 2000–2005 periods and steady bacterial respiration of the particulate and dissolved organic matter coming from surface waters.

During the episodes of local convection at DYFAMED in 1999–2000 and in 2005–2006, there was a mismatch between the OML interruption and deepening of the mixed layer. Such a mismatch had already been observed during the period of deep convection in the Gulf of Lion in 2012/2013, and would be due to a delay between the phases of the convection process and the associated increase in the O_2 content (Coppola et al., 2017). The recent description of the complex convection phases in the northwestern Mediterranean basin (DEWEX experiment) indicated that the deepening of the mixed layer could start slowly before the winter season, become more rapid in January/February, and be followed by rapid stratification in March (Testor et al., 2018). A second mixing event can be triggered if a storm occurs during the weakly stratified phase. Hence the convection phases produce a volume of new ventilated water that varies with the step of the convection event. It follows that monthly observed mixed layer deepening does not perfectly reflect the amount of newly ventilated water formed during each phase of winter convection and thus the related increase in the O_2 content.

Different trends in O_2 concentration in the OML were observed between the two successive episodes of local intense mixing of 1999–2000 and 2005–2006, i.e. an increase between 1999 and 2000 and a decrease between 2005 and 2006 (Fig. 4C). One possible explanation could be a change in the rate of bacterial respiration (microbial activity), due to a difference in the size composition of the phytoplankton community in surface waters. Indeed, the bloom consisted of micro- (mostly diatoms) and nanophytoplankton after the intense convection of winter 1999, and of nanophytoplankton following the intense convection in winter 2005 (Marty and Chiavérini, 2010). The change in plankton size could have affected the efficiency of organic matter export to intermediate water (i.e. higher and faster export after the diatom bloom), and thus the remineralization of phytoplankton-derived sinking organic matter. However, given that monthly MLD measurements can miss some events of short and intense mixing, it is difficult to satisfactorily compare O_2 respiration in intermediate water and phytoplankton bloom composition.

After the WMT event of winter 2005 and the change in LIW properties (i.e. warmer and denser water), there was a decrease in O_2 concentration (Fig. 4C). This could be explained by an increase of isopycnal advection of the core of the LIW (lower O_2 concentrations) to DYFAMED during this period of physical instabilities (Bosse et al., 2015). An additional explanation could be a change in the microbial community, which could have influenced the O_2 respiration efficiency compared to the pre-2005 OML trend. The change in the O_2 respiration rate could have also been caused by remote processes along the LIW track since the WMT event, e.g. a change in the organic matter and nutrients content carried by the LIW along its path from the Levantine basin to the Ligurian Sea. However, only sustained observations in the LIW could provide significant insights to verify such hypothesis.

During the extreme winters of 2004–2005–2006, the water column experienced strong and abrupt events of deep mixing, that causing a rapid decrease in Θ and S (Fig. 4A and B), as reported previously by (Marty and Chiavérini, 2010), reflecting ventilation of the intermediate water in winter 2004/2005 (MLD down to 555 m) and a complete ventilation of the water column in winter 2005/2006 (MLD down to 2300 m) (Fig. 4C). These events removed the typical OML signature for several months (Figs. 3C and 4C), and caused replenishment of O_2 whose concentration in the OML increased by 30–50 $\mu mol\,kg^{-1}$. After the intense deep convection in early 2006, the OML reached its maximum value (200 $\mu mol\,kg^{-1}$), after which it decreased until 2007 without reaching the previous OML value (i.e. 180 instead of 160 $\mu mol\,kg^{-1}$) (Fig. 4C). After warmer winter in 2007 with shallow vertical mixing, the OML developed again in mid-2007, likely as a consequence of the processes discussed above.

The increase in O_2 concentrations in the OML that occurred from December 2012 to July 2013 (from 180 up to 192 $\mu mol\,kg^{-1}$, respectively; Figs. 3C and 4C) is not consistent with the observed monthly MLD at DYFAMED in February 2013 (160 m). However, high frequency measurements from moored sensors at 350 m show that mixing in February-March 2013 was deep enough to supply oxygen to the OML.

In addition, repeated glider transects from Nice to Calvi at this period (Fig. 1; Bosse et al., 2017) showed a deepening of the MLD (down to 800 m) in the Ligurian Sea between 13 and 16 February 2013. This strong, transient deepening of the MLD was likely related to a preceding event of dense water formation in the northwestern basin, which had been observed during the HYMEX SOP2 and DEWEX 1 cruises (Estournel et al., 2016). Also, CTD shipborne observations in the Ligurian Sea during the MOOSE-GE cruise in summer 2013 showed the presence of a homogeneous layer of well-oxygenated water (195–200 μmol kg^{-1}) between 300 and 1200 m (Bosse et al., 2017). This homogeneous layer was associated with a post convective submesoscale coherent vortex (SCV) formed around mid-February 2013 in the Ligurian Sea, which persisted in the area during 4.5 months (Bosse et al., 2017) and could thus explain the progressive increase in the O_2 concentrations observed at DYFAMED from December 2012 to July 2013. This indicates that the post-convective SCV likely affected the O_2 content of the water column over a large area during several months.

Long-term observation of OML variability at DYFAMED indicates that the O_2 minimum persisted despite strong but rare events of vertical winter mixing. If no major replenishment of O_2, from surface to deep waters, occurs in the OML during the coming decades and given the rate of O_2 decrease observed during the periods 1994–1998 and 2000–2005 (loss of 7 and 4 μmol kg^{-1} yr^{-1} from 1994 to 1999 and 2000 to 2005, respectively, i.e. 5 μmol kg^{-1} yr^{-1} on average; Fig. 4C), it would take 25 years to reach a typical O_2 concentration for hypoxia (i.e. 60 μmol kg^{-1}; Gray et al., 2002) from the present 180 μmol kg^{-1}. Given the prediction of climate studies for a possible shallower and more stratified mixed layer in the western Mediterranean Sea in a few decades (Somot et al., 2006), the apparition of a hypoxic oxygen minimum zone in intermediate waters is a possibility that should be considered in biogeochemical and marine ecosystem models.

4.2. Interannual variability of oxygen in the WMDW

In the northwestern Mediterranean Sea, the WMDW results from deep-water formation that mostly occurs offshore in the Gulf of Lion, and in a smaller proportion and less frequently in the Ligurian Sea. Shelf water cascading through the canyons of the Gulf of Lion (Fig. 1) contributes to the formation of dense water and the supply of O_2 to deep waters (Canals et al., 2006; Durrieu de Madron et al., 2013; Puig et al., 2013; Salat, 1995; Touratier et al., 2016; Ulses et al., 2008).

In mid-1994, a very high deep O_2 concentration (212 μmol kg^{-1}; Fig. 5C) was observed at DYFAMED, but this was likely not an effect of local deep mixing because the low local MLD at that time. This observation is consistent with a previous study (Bethoux et al., 2002), where constant deep-water characteristic had been reported for the Ligurian Sea from 1994 to 1998. The very high deep O_2 concentration of 1994 could be explained by the observation of a cold anomaly in the Gulf of Lion in February-March 1994, at a depth of about 1500 m and 100 km downstream of the assumed source in the Gulf of Lion (Send et al., 1996). Given the inferred spreading of about 5 cm s^{-1}, this ventilated deep water could have reached the Ligurian Sea and influenced the deep O_2 concentrations at DYFAMED in mid-1994.

During the period 1995–2004, O_2 concentrations at 2000 m in the WMDW showed a slow decrease, with large seasonal and interannual variability (Fig. 5C). During that period, two events of relatively deep mixing events were observed, i.e. in early 1999 and early 2000, but these reached only 600 and 400 m, respectively (Fig. 5C), as previously reported by Copin-Montégut and Bégovic (2002). Consequently, these events did not affect the deep waters, and the observed slow decrease of O_2 in the WMDW until 2004 likely reflected the lack of deep ventilation and steady bacterial respiration, as in the overlying OML (previous section).

The deep-water O_2 concentrations at DYFAMED stopped decreasing in 2004, i.e. two years before the rapid increase in Θ and S (Fig. 5A–C). This change in the deep-water O_2 trend was coincident with the extensive renewal of the WMDW that started in 2004 in the Gulf of Lion (Schroeder et al., 2008) and likely supplied deep waters with high O_2 concentration to DYFAMED on the same year. The high deep-water O_2 concentration observed in mid-2005 (212 μmol kg^{-1}; Fig. 5C) is not consistent with the earlier local mixing event that had only affected the intermediate water (i.e. MLD of 555 m in winter 2004–2005). However, it coincided with the WMT event that occurred in winter 2004–2005, and the newly formed deep-water mass, which extended from the Gulf of Lion to the Catalan sub-basin, with the production of an unusually and remarkably large volume of deep water. This deep-water formation (DWF) modified the WMDW, which became warmer and saltier (López-Jurado et al., 2005; Schroeder et al., 2006; Canals et al., 2006; Font et al., 2007). It is likely that the accompanying intense deep mixing provided high O_2 concentration to the deep water in the Gulf of Lion, which spread to the Ligurian Sea and affected the local deep O_2 concentration at DYFAMED (with low effect on deep T and S values).

In winter 2005–2006, the DWF occurred mainly in the Ligurian Sea (Smith et al., 2008; Marty and Chiavérini, 2010), resulting in a new WMDW with higher heat and salt contents than the previous year (Fig. 5A and B). The winter 2005–2006 was less severe than the previous winter, with a lower loss of heat from the sea to the atmosphere, and the intense DWF in the Ligurian Sea may have been caused by the presence of a shallow LIW vein (Borghini et al., 2014; Marty and Chiavérini, 2010; Smith et al., 2008; Zunino et al., 2012). The intense formation of deep water in winter 2005–2006 injected a 600 m-thick near-bottom water layer that replaced the old deep water (Schroeder et al., 2016). This event caused the mixing of the whole water column at DYFAMED (Borghini et al., 2014; Marty and Chiavérini, 2010), where a major increase in Θ, S and O_2 at 2000 m occurred in early 2006 (Fig. 5A and B). The new dense (> 29.11 kg m^{-3}) deep water at DYFAMED in spring 2006 was warmer and saltier than the native WMDW, and it had been completely ventilated, with O_2 concentrations up to 15 μmol kg^{-1} higher than in 2004 (Figs. 5–7). During the previous events of deep mixing in the winters of 1999 and 2000, 11 and 15 mol O_2 m^{-2}, respectively, had been introduced in the 0–600 m mixed layer in one month (Bégovic and Copin-Montégut, 2002). These values are smaller than the 24 mol O_2 m^{-2} injected between December 2005 and March 2006, which is consistent with the bottom-reaching convection (and more intense O_2 ventilation) that affected the water column in winter 2005–2006 (Fig. 6). The decrease in the O_2 content after the deep mixing event was rapid, and in April 2006, i.e. one month after the high O_2 ventilation, the water column has lost 9 mol m^{-2} of O_2 (Fig. 6). One explanation to the rapid decrease in deep O_2 may be a rapid spreading of the newly ventilated layer into adjacent deep waters through lateral export and replacement by less oxygenated surrounding waters, as proposed to explain a similar rapid decrease in deep O_2 after an event of deep mixing in the Labrador Sea (Kortzinger et al., 2004).

Two processes could explain the rapid changes that occurred in the WMDW from 2004 to 2006: the winter 2004–2005 was the driest and coldest winter since 1960s (López-Jurado et al., 2005; Schroeder et al., 2006), and the progressive increase in the heat and salt contents of the LIW, which was transferred to the deep water during the two intense DWF of 2004–2005 and 2005–2006. Consequently, it seems that the heat and salt contents of the LIW played a key role during the winters 2004–2005 and 2005–2006. The change in characteristics of the LIW could have been caused by the propagation of the EMT from the Eastern to the Western Mediterranean basin (Schroeder et al., 2006), and/or could have resulted from successive convection events to intermediate depths before winter 2005, which could have caused an increase in heat and salt content in the LIW (Herrmann et al., 2010; Somot et al., 2016).

The change in the LIW characteristics acted as a preconditioning factor that led to intense convection in open waters of the western basin when the external forcing factors (winds and heat loss) were active in winters 2004–2005 and 2005–2006 (Herrmann et al., 2008; Schroeder et al., 2010b). This caused ventilation of the whole water column, which supplied large amounts of O_2 to deep waters. As a result, the

whole resident deep water in the Western basin was replaced by a warmer, saltier and more oxygenated WMDW between 2004 and 2006 (Schroeder et al., 2008).

The observed change in deep O_2 concentrations at DYFAMED from mid-2005 to early 2006 (212 and 208 μmol kg^{-1}, respectively, Fig. 5C) is consistent with the idea that, after the winter 2004–2005, the deep O_2 concentrations at DYFAMED were affected by the spreading of the newly formed WMDW in the Gulf of Lion, while in winter 2005–2006, they were strongly influenced by a local deep mixing event. Concerning the spreading from the Gulf of Lion, Durrieu de Madron et al. (2013) observed that the volume of the newly formed deep water in winter 2012 still increased 5 months after its formation, which could indicate that high O_2 concentrations were preserved in the deep water during its spreading. Concerning the local deep mixing occurred in early 2006, it propagated the LIW and OML signatures into the deep water, which could have slightly reduced the increase in deep O_2 concentrations caused by the spreading of deep water.

Since 2006, the bottom layer has been characterized by the "hook"-shaped Θ-S characteristics with high O_2 concentrations, typical of the new WMDW (Fig. 7; Schroeder et al., 2016). The O_2 concentrations in the new WMDW continued to be high ($\sim$200 μmol kg^{-1}) for more than three years after 2005, with large interannual variability (Fig. 5C), which perhaps reflected the periodical spreading of deep water formed in the Gulf of Lion every winter (Bosse et al., 2015). The winters of 2011, 2012 and 2013 were exceptionally cold in the northwestern Mediterranean, associated with strong surface heat and buoyancy losses that led to intense deep convection. This caused deep vertical mixing and a resulting increase in the heat and salt contents of the deep layer. This event caused an increase in the deep stratification of the bottom water in the Gulf of Lion (Houpert et al., 2016; Schroeder et al., 2016). At the DYFAMED site, a rapid increase in potential temperature and salinity was recorded on mooring at 2000 m during a few weeks in early 2010, 2012 and 2013 (Fig. 5A and B). This suggests that short and intense local deep mixing occurred at DYFAMED, which were not detected by the monthly MLD values. These local events of deep mixing had affected the deep O_2 concentrations since 2010 (Figs. 5C and 7). It is also strongly possible that the newly formed deep water in the Gulf of Lion yearly had spread into the Ligurian Sea, where it had increased the deep O_2 concentrations without any evidence from local observation. The combination of local and remote processes can explain the high deep O_2 variability observed at the DYFAMED site (Fig. 5C).

4.3. Seasonal variability of oxygen in the mixed layer

At the DYFAMED site, the mixing period generally extends from November-December to April, and the stratification period from May to October-November (Fig. 8A), as already described by Copin-Montégut and Bégovic (2002) and Marty et al. (2002). The mean seasonal variation in DO_{MLD} shows a large amplitude of about 40 μmol kg^{-1} (Fig. 8D).

Seasonal changes in DO_{MLD} are related to seasonal changes in both O_2 solubility with temperature and biological production in the mixed layer (Fig. 8D). At the beginning of the mixing period (November-December), O_2 solubility increases as temperature decreases, which promotes O_2 ingassing. When the MLD deepens (January-February), the O_2 taken up from the atmosphere is redistributed over a thicker mixed layer, leading to an undersaturation of the mixed layer (low DO_{MLD}; Fig. 8D). In April, the MLD and O_2 solubility both decrease as temperature increases, which promotes the biological production of O_2. The latter leads to O_2 oversaturation in the mixed layer (maximum DO_{MLD}, Fig. 8D), and the release of O_2 to the atmosphere, i.e. O_2 outgassing. From May to July, the MLD does not change but temperature in the mixed layer continues to increase, and most of the biological production occurs below the MLD. As a consequence, O_2 outgassing is larger than biological O_2 production, leading to a decrease in DO_{MLD} (Fig. 8D).

4.4. Seasonal variability of the oxygen-based NCP

The average seasonal cycle of potential density during the period 1994–2014 shows that the seasonal pycnocline at DYFAMED appears in May, when thermal stratification develops, and disappears in November-December, when the density of surface waters increases during the winter cooling period (Fig. S3A). This seasonal cycle is similar to that of the MLD (Fig. S3A), as expected. The O_2 100% saturation isopleth at DYFAMED never exceeds the depth of 80 m and reaches the surface in winter (from December to the end of February) when cooling promotes mixing of surface and deeper waters (Fig. S3B). The surface water becomes under-saturated in O_2 owing to the cooling and the increase in O_2 solubility (Copin-Montégut and Bégovic, 2002). The O_2 saturation isopleth is deepest from April to November (i.e. below 40 m) during the bloom and stratified period (i.e. shallow MLD). In stratified surface water between April and October, O_2 is often supersaturated (Fig. S3B), likely reflecting the combined effects of strong photosynthesis and limited downward vertical O_2 diffusion (Copin-Montégut and Bégovic, 2002).

The mean annual minimum value of ΔO_2 in the production layer (December-January) coincides with the seasonal deepening of the mixed layer, in December-January (Figs. 8A and 9). There is no ΔO_2 estimate in February because the measured surface O_2 saturation was always < 100% during that month (100% saturation was the threshold used to estimate ΔO_2). In winter, deep mixing (MLD > 100 m) is predominant, and surface water becomes undersaturated in O_2 because of the low temperature, high O_2 solubility, and the entrainment of undersaturated water from the upper into the deep mixed layer. From March to April, ΔO_2 in the production layer increases and reaches its maximum in April. This corresponds to the stratification triggering phytoplankton bloom, as it was observed at DYFAMED (Marty et al., 2002). During this period, photosynthesis increases the production of O_2, which becomes higher than community respiration of O_2, and the increasing stratification may enhance the accumulation of O_2 in surface waters. In December-January, the decrease in ΔO_2 is likely due to the absence of photosynthetic production related to the MLD deepening (together with the limited availability of nutrients and low irradiance during this period) and the predominance of respiration.

The annual mean of NCP (carbon) estimate of 7.1 mol C m^{-2} yr^{-1} (or 85.2 gC m^{-2} yr^{-1}) is higher than the value of 0.4 to 1.5 mol C m^{-2} yr^{-1} estimated by Copin-Montégut (2000) in the upper 40 m of the DYFAMED water column in May 1995. The author's approach was based on continuous measurements of changes in O_2 concentrations during four days and a vertical diffusion model: the measurements had been done in May, and the computed NCP values corresponded to the bloom period. Our NCP estimate is less sophisticated than that of Copin-Montégut (2000), but it is based on long-term measurements that include seasonal and inter-annual variability in O_2 production, and it is not surprising that our estimate is more consistent with the annual new production estimates of Marty and Chiavérini (2002), who measured primary production at DYFAMED monthly during 7 years (1993–1999) using the ^{14}C method. These authors multiplied their values by a phytoplankton pigment-based proxy of the f-ratio to obtain estimates of phytoplankton new production that ranged from 19 to 71 g C m^{-2} yr^{-1}. It must be noted that phytoplankton new production is different from NCP since it does not take into account the consumption of carbon by heterotrophic organisms.

Our NCP estimate of 85.2 g C m^{-2} yr^{-1} is 34 times higher than the mean particulate organic carbon export flux of 2.5 g C m^{-2} yr^{-1} measured in sediment traps deployed at 200 m at DYFAMED during the period 1988–2005 (Miquel et al., 2011). This difference suggests a strong recycling of carbon in the surface layer, i.e. by a factor of 34 between NCP and the export flux. However, if the export of dissolved organic carbon is included (i.e. 18.4 g C m^{-2} yr^{-1} in 1991 and 1992; Avril, 2002; Lefevre et al., 1996), then the factor between our NCP estimate and the total downward carbon export (i.e. particulate and

dissolved) is only 4. This value is within the errors of the various methods. For example, we possibly underestimated the annual NCP values because these were calculated from monthly observations whereas phytoplankton production varies at the daily time scale (Marty and Chiavérini, 2002).

5. Conclusion

Long-term observations at the DYFAMED site showed that the depth of the OML and its O_2 concentrations were deeply modified during five winters over the last 20 years (i.e. 1999, 2000, 2005, 2006 and 2013), corresponding to the deepening of the mixed layer that injected surface O_2 into intermediate and deep waters. During the periods between deep mixing events, isopycnal advection of the core of the LIW and heterotrophic (mostly bacterial) respiration, sustained by seasonal inputs of organic matter from the surface layer, progressively decrease O_2 concentrations and thus strengthened the intensity and the extent of the OML. The long-term observations indicated strong variability in deep-water O_2 concentrations, which were affected by episodic local events of deep ventilation and dense water spreading. Weaker vertical mixing and dense water formation processes are predicted in the northwestern Mediterranean in the coming decades (Somot et al., 2006). If these predictions are correct, the O_2 supply to the intermediate and deep waters could be reduced, transforming the OML into a hypoxic zone with possible effects on marine ecosystems and the carbon cycle.

Acknowledgments

The authors thank the captains and the crews of the N/O Tethys II (CNRS-INSU) and the scientific and technical staff involved in sampling the DYFAMED time series monthly since 1994. The DYFAMED time series has been funded by the CNRS-INSU since 1994, the EMSO network since 2009 (European Research Infrastructure Consortium since September 2016) and the national MOOSE program, which is supported by CNRS-INSU and ALLENVI, since 2010. The present study was supported by the European projects EuroSites (grant No. 202955) and FIXO3 (grant No. 312463) as part of the European Commission's 6th and 7th Framework Programs, respectively, and by funds from UPMC and CNRS to the Laboratoire d'Océanographie de Villefranche.

Appendix A. Supplementary material

Supplementary data associated with this article can be found, in the online version, at http://dx.doi.org/10.1016/j.pocean.2018.03.001.

References

Avril, B., 2002. DOC dynamics in the northwestern Mediterranean Sea (DYFAMED site). Deep Sea Res. Part II 49, 2163–2182.
Bégovic, M., Copin-Montégut, C., 2002. Processes controlling annual variations in the partial pressure of CO_2 in surface waters of the central northwestern Mediterranean Sea (Dyfamed site). Deep Sea Res. Part II 49, 2031–2047.
Bethoux, J.P., Prieur, L., Nyffeler, F., 1982. The Water Circulation in the North-Western Mediterranean Sea, its Relations with Wind and Atmospheric Pressure. In: Nihoul, J. C.J. (Ed.), Elsevier Oceanography Series, Hydrodynamics of Semi-Enclosed Seas, vol. 34, pp. 129–142.
Bethoux, J.P., Prieur, L., 1983. Hydrologie et circulation en Méditerranée Nord-Occidentale. Editions Technip. Pétroles et techniques 299, 25–34.
Bethoux, J.P., Durieu de Madron, X., Nyffeler, F., Tailliez, D., 2002. Deep water in the western Mediterranean: peculiar 1999 and 2000 characteristics, shelf formation hypothesis, variability since 1970 and geochemical inferences. J. Mar. Syst. 33–34, 117–131.
Borghini, M., Bryden, H., Schroeder, K., Sparnocchia, S., Vetrano, A., 2014. The Mediterranean is becoming saltier. Ocean Sci. 10, 693–700.
Bosse, A., Testor, P., Mayot, N., Prieur, L., D'Ortenzio, F., Mortier, L., Le Goff, H., Gourcuff, C., Coppola, L., Lavigne, H., Raimbault, P., 2017. A submesoscale coherent vortex in the Ligurian Sea: from dynamical barriers to biological implications. J. Geophys. Res. Oceans.
Bosse, A., Testor, P., Mortier, L., Prieur, L., Taillandier, V., d'Ortenzio, F., Coppola, L., 2015. Spreading of Levantine Intermediate Waters by submesoscale coherent vortices in the northwestern Mediterranean Sea as observed with gliders. J. Geophys. Res. Oceans 120, 1599–1622.
Canals, M., Puig, P., de Madron, X.D., Heussner, S., Palanques, A., Fabres, J., 2006. Flushing submarine canyons. Nature 444, 354–357.
Cianca, A., Santana, R., Hartman, S.E., Martín-González, J.M., González-Dávila, M., Rueda, M.J., Llinás, O., Neuer, S., 2013. Oxygen dynamics in the North Atlantic subtropical gyre. Deep Sea Res. Part II 93, 135–147.
Copin-Montégut, C., 2000. Consumption and production on scales of a few days of inorganic carbon, nitrate and oxygen by the planktonic community: results of continuous measurements at the Dyfamed Station in the northwestern Mediterranean Sea (May 1995). Deep Sea Res. Part I 47, 447–477.
Copin-Montégut, G., Avril, B., 1993. Vertical distribution and temporal variation of dissolved organic carbon in the North-Western Mediterranean Sea. Deep Sea Res. Part I 40, 1963–1972.
Copin-Montégut, C., Bégovic, M., 2002. Distributions of carbonate properties and oxygen along the water column (0–2000 m) in the central part of the NW Mediterranean Sea (Dyfamed site): influence of winter vertical mixing on air–sea CO_2 and O_2 exchanges. Deep Sea Res. Part II 49, 2049–2066.
Coppola, L., Diamond Riquier, E., Carval, T., 2016. Dyfamed Observatory Data. SEANOE.
Coppola, L., Prieur, L., Taupier-Letage, I., Estournel, C., Testor, P., Lefevre, D., Belamari, S., LeReste, S., Taillandier, V., 2017. Observation of oxygen ventilation into deep waters through targeted deployment of multiple Argo-O_2 floats in the north-western Mediterranean Sea in 2013. J. Geophys. Res. Oceans 122, 6325–6341.
D'Ortenzio, F., Ludicone, D., de Boyer Montegut, C., Testor, P., Antoine, D., Marullo, S., Santoleri, R., Madec, G., 2005. Seasonal variability of the mixed layer depth in the Mediterranean Sea as derived from in situ profiles. Geophys. Res. Lett. 32.
de Boyer Montégut, C., 2004. Mixed layer depth over the global ocean: an examination of profile data and a profile-based climatology. J. Geophys. Res. 109.
Durrieu de Madron, X., Houpert, L., Puig, P., Sanchez-Vidal, A., Testor, P., Bosse, A., Estournel, C., Somot, S., Bourrin, F., Bouin, M.N., Beauverger, M., Beguery, L., Calafat, A., Canals, M., Cassou, C., Coppola, L., Dausse, D., D'Ortenzio, F., Font, J., Heussner, S., Kunesch, S., Lefevre, D., Le Goff, H., Martín, J., Mortier, L., Palanques, A., Raimbault, P., 2013. Interaction of dense shelf water cascading and open-sea convection in the northwestern Mediterranean during winter 2012. Geophys. Res. Lett. 40, 1379–1385.
Emerson, S., Bushinsky, S., 2014. Oxygen concentrations and biological fluxes in the open ocean. Oceanography 27, 168–171.
Emerson, S., Quay, P.D., Stump, C., Wilbur, D., Schudlich, R., 1995. Chemical tracers of productivity and respiration in the subtropical Pacific Ocean. J. Geophys. Res. 100, 15873.
Estournel, C., Testor, P., Damien, P., D'Ortenzio, F., Marsaleix, P., Conan, P., Kessouri, F., Durrieu de Madron, X., Coppola, L., Lellouche, J.-M., Belamari, S., Mortier, L., Ulses, C., Bouin, M.-N., Prieur, L., 2016. High resolution modeling of dense water formation in the north-western Mediterranean during winter 2012–2013: processes and budget. J. Geophys. Res. Oceans 121, 5367–5392.
Font, J., Puig, P., Salat, J., Palanques, A., Emelianov, M., 2007. Sequence of hydrographic changes in NW Mediterranean deep water due to the exceptional winter of 2005. Sci. Mar. 71 (2), 339–346.
Gasparini, G.P., Ortona, A., Budillon, G., Astraldi, M., Sansone, E., 2005. The effect of the Eastern Mediterranean Transient on the hydrographic characteristics in the Strait of Sicily and in the Tyrrhenian Sea. Deep Sea Res. Part I 52, 915–935.
Gray, J.S., Wu, R.S., Or, Y.Y., 2002. Effects of hypoxia and organic enrichment on the coastal marine environment. Mar. Ecol. Prog. Ser. 238, 249–279.
Herrmann, M., Sevault, F., Beuvier, J., Somot, S., 2010. What induced the exceptional 2005 convection event in the northwestern Mediterranean basin? Answers from a modeling study. J. Geophys. Res. 115.
Herrmann, M., Somot, S., Sevault, F., Estournel, C., Déqué, M., 2008. Modeling the deep convection in the northwestern Mediterranean Sea using an eddy-permitting and an eddy-resolving model: case study of winter 1986–1987. J. Geophys. Res. 113.
Ho, D.T., Law, C.S., Smith, M.J., Schlosser, P., Harvey, M., Hill, P., 2006. Measurements of air-sea gas exchange at high wind speeds in the Southern Ocean: implications for global parameterizations. Geophys. Res. Lett. 33.
Houpert, L., Durrieu de Madron, X., Testor, P., Bosse, A., D'Ortenzio, F., Bouin, M.N., Dausse, D., Le Goff, H., Kunesch, S., Labaste, M., Coppola, L., Mortier, L., Raimbault, P., 2016. Observations of open-ocean deep convection in the northwestern Mediterranean Sea: Seasonal and interannual variability of mixing and deep water masses for the 2007–2013 Period. J. Geophys. Res. Oceans 121, 8139–8171.
Janzen, C., Murphy, D., Larson, N., 2007. Getting more mileage out of dissolved oxygen sensors in long-term moored applications. 2007 Oceans, vols. 1–5, pp. 1889–1893.
Jenkins, W.J., Goldman, J.C., 1985. Seasonal oxygen cycling and primary production in the Sargasso Sea. J. Mar. Res. 43, 465–491.
Karl, D.M., Michaels, A.F., 1996. The Hawaiian Ocean Time-series (HOT) and Bermuda Atlantic Time-series study (BATS). Deep Sea Res. Part II 43, 127–128.
Klein, B., Roether, W., Manca, B.B., Bregant, D., Beitzel, V., Kovacevic, V., Luchetta, A., 1999. The large deep water transient in the Eastern Mediterranean. Deep Sea Res. Part I 46, 371–414.
Kortzinger, A., Schimanski, J., Send, U., Wallace, D., 2004. The ocean takes a deep breath. Science 306, 1337.
Lascaratos, A., Roether, W., Nittis, K., Klein, B., 1999. Recent changes in deep water formation and spreading in the eastern Mediterranean Sea: a review. Prog. Oceanogr. 44, 5–36.
Lefevre, D., Denis, M., Lambert, C.E., Miquel, J.C., 1996. Is DOC the main source of organic matter remineralization in the ocean water column? J. Mar. Syst. 7, 281–291.
López-Jurado, J.L., González-Pola, C., Vélez-Belchí, P., 2005. Observation of an abrupt disruption of the long-term warming trend at the Balearic Sea, western Mediterranean Sea, in summer 2005. Geophys. Res. Lett. 32.
Malanotte-Rizzoli, P., Manca, B.B., d'Alcala, M.R., Theocharis, A., Brenner, S., Budillon,

G., Ozsoy, E., 1999. The Eastern Mediterranean in the 80s and in the 90s: the big transition in the intermediate and deep circulations. Dyn. Atmos. Oceans 29, 365–395.
Marty, J.-C., Chiavérini, J., 2002. Seasonal and interannual variations in phytoplankton production at DYFAMED time-series station, northwestern Mediterranean Sea. Deep Sea Res. Part II 49, 2017–2030.
Marty, J.-C., Chiavérini, J., Pizay, M.-D., Avril, B., 2002. Seasonal and interannual dynamics of nutrients and phytoplankton pigments in the western Mediterranean Sea at the DYFAMED time-series station (1991–1999). Deep Sea Res. Part II 49, 1965–1985.
Marty, J.C., 2002. The DYFAMED time-series program (French-JGOFS) - Preface. Deep-Sea Res. Part Ii-Top. Stud. Oceanogr. 49, 1963–1964.
Marty, J.C., Chiavérini, J., 2010. Hydrological changes in the Ligurian Sea (NW Mediterranean, DYFAMED site) during 1995–2007 and biogeochemical consequences. Biogeosciences 7, 2117–2128.
Millot, C., Taupier-Letage, I., 2005. Circulation in the Mediterranean Sea. In: In: Saliot, A. (Ed.), The Mediterranean Sea, vol. 5K. Springer, Berlin Heidelberg, pp. 29–66.
Miquel, J.-C., Martín, J., Gasser, B., Rodriguez-y-Baena, A., Toubal, T., Fowler, S.W., 2011. Dynamics of particle flux and carbon export in the northwestern Mediterranean Sea: a two decade time-series study at the DYFAMED site. Prog. Oceanogr. 91, 461–481.
Najjar, R.G., Keeling, R.F., 1997. Analysis of the mean annual cycle of the dissolved oxygen anomaly in the World Ocean. J. Mar. Res. 55, 117–151.
Nilsen, J.E.Ø., Falck, E., 2006. Variations of mixed layer properties in the Norwegian Sea for the period 1948–1999. Prog. Oceanogr. 70, 58–90.
Packard, T.T., Minas, H.J., Coste, B., Martinez, R., Bonin, M.C., Gostan, J., Garfield, P., Christensen, J., Dortch, Q., Minas, M., Copinmontegut, G., Copinmontegut, C., 1988. Formation of the Alboran Oxygen Minimum Zone. Deep-Sea Res. Part A-Oceanogr. Res. Pap. 35, 1111–1118.
Pasqueron de Fommervault, O., Migon, C., D'Ortenzio, F., Ribera d'Alcalà, M., Coppola, L., 2015. Temporal variability of nutrient concentrations in the northwestern Mediterranean sea (DYFAMED time-series station). Deep Sea Res. Part I 100, 1–12.
Prieur, L., Bethoux, J.P., Bong, J.H., Tailliez, D., 1983. Particularités hydrologiques et formation d'eau profonde dans le bassin Liguro-provençal en 1981–1982. Rapp. Comm. Int. Mer Médit. 28 (2), 51–53.
Puig, P., Madron, X.D.d., Salat, J., Schroeder, K., Martín, J., Karageorgis, A.P., Palanques, A., Roullier, F., López-Jurado, J.L., Emelianov, M., Moutin, T., Houpert, L., 2013. Thick bottom nepheloid layers in the western Mediterranean generated by deep dense shelf water cascading. Prog. Oceanogr. 111, 1–23.
Redfield, A.C., Ketchum, B.H., Richards, F.A., 1963. The influence of organisms on the composition of seawater, p. 26–77. In: Hill, M.N. (Ed.), The sea, v. 2. Interscience.
Riser, S.C., Johnson, K.S., 2008. Net production of oxygen in the subtropical ocean. Nature 451, 323–325.
Roether, W., Klein, B., Beitzel, V., Manca, B.B., 1998. Property distributions and transient-tracer ages in Levantine Intermediate Water in the Eastern Mediterranean. J. Mar. Syst. 18, 71–87.
Roether, W., Schlitzer, R., 1991. Eastern Mediterranean deep water renewal on the basis of chlorofluoromethane and tritium data. Dyn. Atmos. Oceans 15, 333–354.
Salat, J., 1995. Review of hydrographic environmental factors that may influence anchovy habitats in northwestern Mediterranean. SCIENTIA MARINA 60, 21–32.
Schneider, A., Tanhua, T., Roether, W., Steinfeldt, R., 2014. Changes in ventilation of the Mediterranean Sea during the past 25 year. Ocean Sci. 10, 1–16.
Schroeder, K., Chiggiato, J., Bryden, H.L., Borghini, M., Ben Ismail, S., 2016. Abrupt climate shift in the Western Mediterranean Sea. Sci Rep 6, 23009.
Schroeder, K., Gasparini, G.P., Borghini, M., Cerrati, G., Delfanti, R., 2010a. Biogeochemical tracers and fluxes in the Western Mediterranean Sea, spring 2005. J. Mar. Syst. 80, 8–24.
Schroeder, K., Gasparini, G.P., Tangherlini, M., Astraldi, M., 2006. Deep and intermediate water in the western Mediterranean under the influence of the Eastern Mediterranean Transient. Geophys. Res. Lett. 33.
Schroeder, K., Josey, S.A., Herrmann, M., Grignon, L., Gasparini, G.P., Bryden, H.L., 2010b. Abrupt warming and salting of the Western Mediterranean Deep Water after 2005: atmospheric forcings and lateral advection. J. Geophys. Res. 115.
Schroeder, K., Millot, C., Bengara, L., Ben Ismail, S., Bensi, M., Borghini, M., Budillon, G., Cardin, V., Coppola, L., Curtil, C., Drago, A., El Moumni, B., Font, J., Fuda, J.L., García-Lafuente, J., Gasparini, G.P., Kontoyiannis, H., Lefevre, D., Puig, P., Raimbault, P., Rougier, G., Salat, J., Sammari, C., Sánchez Garrido, J.C., Sanchez-Roman, A., Sparnocchia, S., Tamburini, C., Taupier-Letage, I., Theocharis, A., Vargas-Yáñez, M., Vetrano, A., 2013. Long-term monitoring programme of the hydrological variability in the Mediterranean Sea: a first overview of the HYDROCHANGES network. Ocean Sci. 9, 301–324.
Schroeder, K., Ribotti, A., Borghini, M., Sorgente, R., Perilli, A., Gasparini, G.P., 2008. An extensive western Mediterranean deep water renewal between 2004 and 2006. Geophys. Res. Lett. 35.
Send, U., Mertens, C., Font, J., 1996. Recent observation indicates convection' role in deep water circulation. Eos, Trans. Am. Geophys. Union 77.
Smith, R.O., Bryden, H.L., Stansfield, K., 2008. Observations of new western Mediterranean deep water formation using Argo floats 2004–2006. Ocean Sci. 4, 133–149.
Somot, S., Houpert, L., Sevault, F., Testor, P., Bosse, A., Taupier-Letage, I., Bouin, M.-N., Waldman, R., Cassou, C., Sanchez-Gomez, E., Durrieu de Madron, X., Adloff, F., Nabat, P., Herrmann, M., 2016. Characterizing, modelling and understanding the climate variability of the deep water formation in the North-Western Mediterranean Sea. Clim. Dyn.
Somot, S., Sevault, F., Déqué, M., 2006. Transient climate change scenario simulation of the Mediterranean Sea for the twenty-first century using a high-resolution ocean circulation model. Clim. Dyn. 27, 851–879.
Tanhua, T., Hainbucher, D., Schroeder, K., Cardin, V., Álvarez, M., Civitarese, G., 2013. The Mediterranean Sea system: a review and an introduction to the special issue. Ocean Sci. 9, 789–803.
Testor, P., Bosse, A., Houpert, L., Margirier, F., Mortier, L., Legoff, H., Dausse, D., Labaste, M., Karstensen, J., Hayes, D., Olita, A., Ribotti, A., Schroeder, K., Chiggiato, J., Onken, R., Heslop, E., Mourre, B., D'Ortenzio, F., Mayot, N., Lavigne, H., de Fommervault, O., Coppola, L., Prieur, L., Taillandier, V., Durrieu de Madron, X., Bourrin, F., Many, G., Damien, P., Estournel, C., Marsaleix, P., Taupier-Letage, I., Raimbault, P., Waldman, R., Bouin, M.-N., Giordani, H., Caniaux, G., Somot, S., Ducrocq, V., Conan, P., 2018. Multiscale Observations of Deep Convection in the Northwestern Mediterranean Sea during Winter 2012–2013 Using Multiple Platforms. J. Geophys. Res.: Ocea.
Touratier, F., Goyet, C., Houpert, L., de Madron, X.D., Lefèvre, D., Stabholz, M., Guglielmi, V., 2016. Role of deep convection on anthropogenic CO2 sequestration in the Gulf of Lions (northwestern Mediterranean Sea). Deep Sea Res. Part I 113, 33–48.
Uchida, H., Johnson, G.C., McTaggart, K.E., 2010. CTD oxygen sensor calibration procedures. In I.R. 14 (Ed.), The GO-SHIP Repeat Hydrography Manual: A Collection of Expert Reports and Guidelines.
Ulses, C., Estournel, C., Puig, P., Durrieu de Madron, X., Marsaleix, P., 2008. Dense shelf water cascading in the northwestern Mediterranean during the cold winter 2005: quantification of the export through the Gulf of Lion and the Catalan margin. Geophys. Res. Lett. 35, L07610.
Winkler, L.W., 1888. Die Bestimmung des im Wasser gelösten Sauerstoffes. Berichte der deutschen chemischen Gesellschaft 21, 2843–2854.
Zunino, P., Schroeder, K., Vargas-Yáñez, M., Gasparini, G.P., Coppola, L., García-Martínez, M.C., Moya-Ruiz, F., 2012. Effects of the Western Mediterranean Transition on the resident water masses: pure warming, pure freshening and pure heaving. J. Mar. Syst. 96–97, 15–23.